



GEOSCIENCES

On the potential of glaciochemical analysis of Joinville Island firn core for the sea ice reconstruction around the northern Antarctic Peninsula

ALEXANDRE S. DE ALENCAR, HEITOR EVANGELISTA, SÉRGIO J. GONÇALVES JR, JEFFERSON C. SIMÕES, ISRAEL FELZENSZWALB, ALBERTO SETZER & HEBER R. PASSOS

Abstract: The Antarctic Peninsula is undergoing rapid climate changes, impacting its surrounding marine ecosystem. At that site, sea ice plays a crucial role in this ecosystem by serving as a habitat for organisms and influencing primary productivity. Studying sea ice variability and primary productivity is essential for understanding environmental changes in Antarctica. This research focused on Joinville Island, located at the tip of the Antarctic Peninsula, where meteorological data and glaciochemical analysis were conducted on snow/firn cores for Cl^- , Na^+ , Ca^{2+} , Mg^{2+} , SO_4^{2-} , NO_3^- , K^+ , MSA, NH_4^+ and F to retrieve recent past environmental variabilities. The study revealed that Joinville Island experienced a net accumulation rate of 0.40 meters per year in water equivalent between 1993 and 2005. In snow/firn cores, Na^+ correlated with both wind strength and sea ice extent ($r=0.59$ and $r=0.66$, respectively) while correlations were higher for MSA and Cl^- with respect to sea ice ($r=0.80$ and $r=0.74$, respectively), considering both the Weddell and Amundsen-Bellinghshausen sub-sectors. This analysis contributes to our understanding of sea ice dynamics and its influence on primary productivity in the area.

Key words: Antarctica, glaciochemistry, snow/firn core, Primary production, MSA.

INTRODUCTION

The Antarctic Peninsula is experiencing rapid warming, increasing air and sea temperatures, and changes in precipitation patterns (Vaughan et al. 2003). These changes have significant implications for the marine ecosystem, particularly for sea ice dynamics and primary productivity (Ducklow et al. 2007, Montes-Hugo et al. 2009). Sea ice is essential for providing habitat, regulating light availability, and influencing nutrient fluxes, ultimately affecting the entire ecosystem's productivity (Arrigo & van Dijken 2015).

The cryosphere, which includes all-natural snow and ice on Earth, plays a crucial role in

the global climate system due to its impact on surface albedo and heat exchange between the atmosphere and the underlying terrestrial or marine environments. Antarctica and Greenland ice sheets are the primary contributors to the current ice cover, and polar regions have been identified as valuable natural observatories of climate change. However, the rise in global temperatures over the past decades threatens these ice deposits and their important records of climatic history (Alley et al. 2001).

Some recent studies indicate a decline in sea ice extent in the Weddell Sea region, a critical part of the Southern Ocean (Zemp et al. 2019, Jena et al. 2022). In 2022, satellite measurements

revealed that sea ice levels in the Weddell Sea were the lowest on record, highlighting the rapid changes occurring in the polar regions due to climate change (Jena et al. 2022, Turner et al. 2022, Wang et al. 2022). The decline of sea ice in this area has significant implications for the delicate ecosystems and wildlife that rely on this habitat for survival, such as penguins, seals, and krill. This alarming trend underscores the urgent need for global action to mitigate greenhouse gas emissions and address the underlying causes of climate change (IPCC 2022). By understanding and addressing the drivers of this decline, we can strive toward a more sustainable and resilient future for our planet.

The impacts of climate change are widespread across the planet, with over 80% of observed transformations aligning with warming trends (IPCC 2022). The Antarctic Peninsula has experienced significant temperature increases and substantial changes in physical and biological systems, which can have far-reaching effects through teleconnections (Turner et al. 2016). Indirect indicators, known as proxies, are crucial in reconstructing past climatic signatures and understanding environmental changes over time. The polar regions are particularly valuable for preserving atmospheric gases and other compounds within their ice layers, making them invaluable environmental reservoirs for long-term records. Glaciochemical analysis of snow and ice cores has become a powerful tool for reconstructing past environmental conditions and understanding long-term trends. Chemical composition analysis of these cores provides insights into the history of sea ice variability and primary productivity in a specific region (Mayewski et al. 1994).

Sea ice in the Weddell Sea and the northern region of the Antarctic Peninsula plays a crucial role in the production of the compound methanesulfonic acid (MSA, $\text{CH}_3\text{SO}_3\text{H}$) and its

subsequent impact on primary production and its relationship with krill (Massom & Stammerjohn 2010, Abram et al. 2013). MSA is a byproduct of oxidation reactions in the atmosphere subsequent to dimethylsulfoniopropionate (DMSP) production by certain species of phytoplankton (Becagli et al. 2019). The primary source of MSA is the oxidation of dimethyl sulfide (DMS), a volatile sulfur compound produced by phytoplankton (Read et al. 2008). DMS is oxidized in the atmosphere to form MSA and sulfate through complex multiphase photochemical reactions (Rasmussen et al. 2022). This process occurs primarily in coastal and oceanic regions, where DMS emissions are prevalent (Johnson & Jen 2023). The oxidation of DMS to MSA occurs through both gas-phase and aqueous-phase reactions, with the latter resulting in the formation of dimethyl sulfoxide (DMSO) and subsequent MSA (Müller et al. 2019). Furthermore, MSA and its salts accumulate near the aerosol surface, making them available for heterogeneous oxidation at the gas-aerosol interface by oxidants such as hydroxyl radicals (Kwong et al. 2018).

The significance of MSA lies in its role as a biogenic sulfur aerosol and a stable oxidation product of DMS, which contributes to the formation of molecular clusters in the marine atmosphere (Benmergui et al. 2012, Rasmussen et al. 2022). Additionally, MSA is a crucial component in the marine sulfur cycle, as it is rapidly oxidized by hydroxyl radicals in the atmosphere, leading to the formation of new particles and cloud condensation nuclei (Marbouti et al. in press). This process has implications for weather and climate, as MSA oxidation products participate in forming cloud condensation nuclei, influencing global radiation balance (Yu et al. 2019).

MSA release into the surrounding waters acts as a natural fertilizer, stimulating the growth of phytoplankton and other microorganisms (Arrigo

& van Dijken 2003). The phytoplankton supports the entire marine food web, with krill being a key component (Kawaguchi et al. 2005). As primary consumers, krill heavily rely on the availability of phytoplankton as their main food source (Arrigo et al. 2017). The relationship between sea ice and phytoplankton development is crucial in understanding the potential impact of climate change on MSA production and its subsequent effects on primary production and the krill population. Sea ice plays a significant role in structuring Antarctic ecosystems, particularly in influencing phytoplankton dynamics and primary production (Eicken 1993). Evidence suggests that under-ice phytoplankton blooms may be more widespread over nutrient-rich Arctic continental shelves, and satellite-based estimates of annual primary production in these waters may be underestimated by up to 10-fold (Arrigo et al. 2012). Furthermore, fully consolidated sea ice has been observed to support modest under-ice blooms, while waters beneath sea ice with leads had significantly lower phytoplankton biomass, despite high nutrient availability (Lowry et al. 2018)

The decline of sea ice due to climate change can have profound implications for phytoplankton development and primary production. Simulations have highlighted those environmental processes such as the fall phytoplankton decline, sea ice advance, and the development of sea ice microbial communities, as well as the late winter increase in sea ice microbial community biomass, control food availability and the physiological condition of krill (Lowe et al. 2012).

The presence of sea ice also influences the size structure and biomass of phytoplankton communities during the spring bloom period. Furthermore, sea ice-associated phytoplankton blooms can critically impact the food web structure, from lower trophic level production to

marine fisheries (Jin et al. 2007). Understanding and monitoring these interactions is crucial for comprehending the broader implications of climate change on the delicate Antarctic ecosystem and implementing effective conservation measures (Kawaguchi et al. 2013).

Marine primary productivity refers to converting inorganic carbon into organic matter through photosynthesis in the marine environment, whereas phytoplankton is responsible for approximately 95% of this productivity (Falkowski et al. 1998). Marine primary productivity plays an important role in biogeochemical cycles and energy flow in the oceans. Various environmental factors, such as light intensity, nutrient availability, and physical mechanisms, influence marine primary productivity in a region. The concentration and/or flux of MSA is an indicator of marine biological activity and has been used in paleoclimatological studies. It can be transported over long distances, affecting the radiation balance in the atmosphere-land system (Andreae & Crutzen 1997). Studies have shown correlations between MSA concentration and the extent of sea ice in Antarctica (Curran et al. 2003), indicating that the coastal region of Antarctica shows different results in terms of marine primary productivity compared to the continental region.

The dating of stratigraphic layers in snow and ice cores is achieved through various methods, including compound concentration analysis, identification of reference horizons, and depth-age models (Svensson et al. 2006). Studies have significantly contributed to glaciology advancements and understanding of past climate changes (Thomas et al. 2013, Mulvaney et al. 2012, Roberts et al. 2017).

Joinville Island, located on the western side of the Antarctic Peninsula, is an ideal location for such investigations due to its proximity to key oceanographic features and accessibility

to scientific research. Based on the hypothesis that the reconstruction of sea ice variability and primary ocean productivity in the Antarctic Peninsula region can be achieved through the study of consistent indirect indicators (proxies) deposited in ice core samples from locations in this region, the main objectives here are to investigate the atmospheric record represented by the snow/firn core deposits on Joinville Island through the analysis of chemical and physical variations. By investigating and utilizing the glaciochemical record of MSA, chloride (Cl⁻), and sodium (Na⁺) in the study of sea ice variability and primary ocean productivity in the Antarctic Peninsula region, this study aims to determine whether these proxies are representative of the variability of sea ice and ocean primary productivity in the Antarctic Peninsula region.

Abbreviations

Amundsen-Bellingshausen Seas (ABS)
 Cold Regions Research Engineering Laboratory, U.S. Army Corps of Engineers (CRREL)
 National Space Institute of Brazil (INPE)
 Institut des Géosciences de l'Environnement (IGE)
 James Ross Island (JRI)
 King George Island (KGI)
 Laboratoire de Glaciologie et Géophysique de l'Environnement (LGGE)
 Laboratoire des Sciences du Climat et de l'Environnement (LSCE)
 Laboratoire des Sciences du Climat et de l'Environnement (LSCE)
 North Amundsen-Bellingshausen sector (BN)
 North Weddell sector (WN)
 Brazilian Antarctic Program (PROANTAR)
 South Amundsen-Bellingshausen sector (BS)
 South Weddell sector (WS)
 WS Joinv. (wind speed on Joinville Island)
 Southern Weddell Sea (W)

MATERIALS AND METHODS

Sampling procedure and location site

The samples were collected at the first Brazilian Glaciological Expedition to Joinville Island during the Austral summer (17 November to 14 December 2005) (Brazilian OPERANTAR XXIV) supported by PROANTAR (Brazilian Antarctic Program). A base camp was established (63°11'19.1" S, 55°23'28.8" W) on a plateau 70 meters above sea level. Figure 1 shows the sampling site.

Two snow/firn cores named TG1 (63°15'17.8" S, 55°38'20.6" W) and TG2 (63°15'17.8" S, 55°38'20.6" W), reaching approximately 8 m and 5 m deep, respectively, were obtained using a portable SIPRE auger manufactured by the CRREL (Cold Regions Research Engineering Laboratory, U.S. Army Corps of Engineers). TG1 and TG2 were retrieved at 565 m and 454 m above sea level, respectively.

Sections of 1 m were cut from the cores then we proceed with visual stratigraphic description (i.e. without the aid of a light table or any magnification instrument) and density measurement. Each section was cut into independent samples every 10 cm of depth using a surgical steel saw. In clean laboratory conditions, the samples underwent surface mechanical decontamination by scraping the outer surface with a plastic saw, were weighed using a mechanical balance (precision of ± 10%), placed in polyethylene containers, labeled, and finally stored in Styrofoam or plastic boxes for subsequent transportation. All tools and the containers used for sample storage were previously decontaminated in the laboratory using ultrapure water (Milli-Q). High-density polyethylene cylindrical containers (height: 12.5 cm, width: 11 cm, volume: 11 cm³) were used for storing the collected samples, which were previously cleaned in the laboratory. After cleaning, they were placed in a vertical laminar flow chamber model PA320, class 100 (ABNT

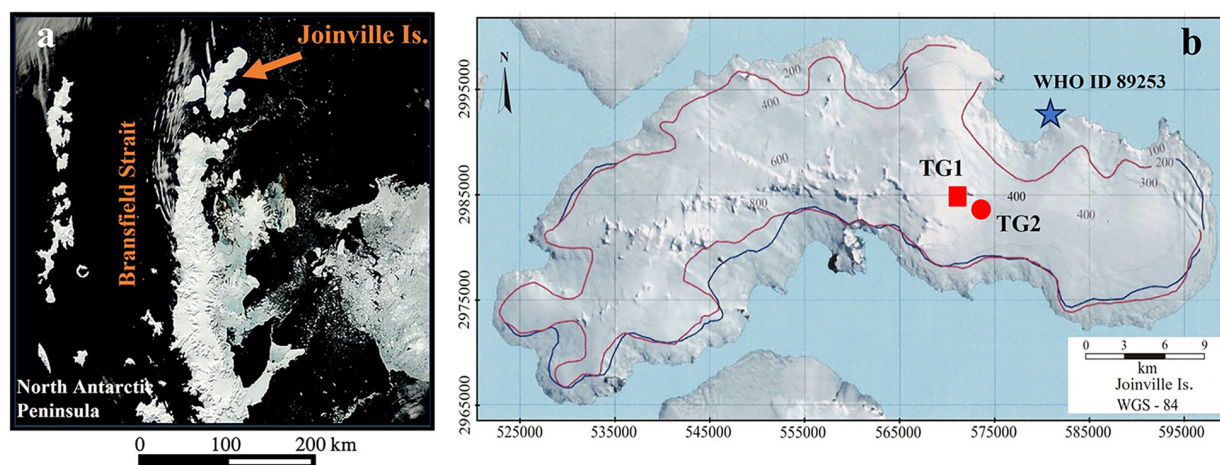


Figure 1. a) Map indicating Joinville Island (Adapted from the NASA Earth Observatory/the MODIS Rapid Response Team at NASA GSFC/Public domain Usage) and b) the location of sampling points (TG1 and TG2) of snow/firn cores and WMO weather station, whereas the snow line altitude variation was indicated by the blue line, representing the snow line height in 1990 and the red line indicates the snow in 2000.

1996) for drying and subsequent preparation for transport to the sampling point.

After sampling, the samples were transported to the laboratory under carefully controlled conditions to prevent contamination and maintain their integrity. Quality control measures were implemented throughout the samples and analysis to ensure accurate and reliable results. Calibration standards, blanks, and replicate samples were included to assess measurement precision and detect potential contamination sources.

Ion Concentration Analysis

The samples were transported to the LGGE, handled in a clean room, and prepared for subsequent analyses. Approximately 95% of the samples remained preserved in a solid state until their analysis, maintaining the same conformation as when they were taken from the Joinville Island ice cap, while the remaining 5% experienced partial thawing during transport. At LGGE, the samples were stored in a cold chamber at -15°C .

Major ions present in the snow/firn cores, such as Cl^- , sulfate (SO_4^{2-}), nitrate (NO_3^-), and Na^+ , were measured using ion chromatography. These measurements provide insights into the sources of chemical compounds and atmospheric deposition. The samples were only melted and opened in a clean room, and sample aliquots were separated under a class 100 laminar flow bench. Precautions such as wearing antistatic clothing and changing sterile vinyl gloves were taken to minimize sample contamination. The two-chromatography system used in this study consisted of DIONEX chromatographs (models DX300 and DX600) conducted at the Laboratoire de Glaciologie et Géophysique de l'Environnement (LGGE), presently the Institut des Géosciences de l'Environnement (IGE), Grenoble, France. The DX300 chromatograph was used for the analysis of cations: Na^+ , NH_4^+ (Ammonium), K^+ (Potassium), Mg^{2+} (Magnesium), and Ca^{2+} (Calcium). The DX600 was used for the analysis of anions: F^- (Fluoride), MSA , Cl^- , NO_3^- , and SO_4^{2-} .

Isotopic Analysis

Stable isotopic ratios that constitute the ice crystals indicate sea ice extent changes, surface temperature, and distance from the moisture source. We measured the oxygen isotope ratio ($d^{18}\text{O}$) of access environmental conditions at the cores site. The snow/firn core samples were opened and thawed in a clean room. A 15 mL aliquot from each TG1 and TG2 core was separated for isotopic analysis at Laboratoire des Sciences du Climat et de l'Environnement (LSCE) in Gif-Sur-Yvette, Paris, France. These samples were stored in a cold chamber at -25°C until analysis. After thawing under a class 100 laminar flow hood, a 3 mL volume was extracted from each sub-sample for isotopic analysis. The $^{18}\text{O}/^{16}\text{O}$ ($d^{18}\text{O}$) (Dansgaard 1964) ratio analysis was performed using a Finnigan MAT 252 mass spectrometer with two equilibration units. After instrumental corrections, the associated error in $d^{18}\text{O}$ concentration calculation in the samples was $\pm 0.05\%$.

Local Climatology

The meteorological data from Joinville Island were obtained from the automatic weather station WMO ID 89253 ($63^{\circ}10'58.8''\text{S}$, $55^{\circ}24'00.0''\text{W}$; elevation: 75 meters) from 1997 to 2003, except for 1998, when it was inoperative due to a technical problem. The Meteorology Project of INPE (National Space Institute of Brazil, <http://antartica.cptec.inpe.br/>) operated the station at the time within PROANTAR. The data analysis showed that the mean air temperature in Joinville Island during the above period was $-5.4 \pm 6.4^{\circ}\text{C}$, with a minimum temperature of -28.2°C occurring in 2002 and a maximum of 8.7°C in 2003. During the same period, the average wind speed was $10.1 \pm 7.2 \text{ m s}^{-1}$ ($\sim 36 \text{ km h}^{-1}$), with gusts reaching a maximum value of 66.7 m s^{-1} ($\sim 240 \text{ km h}^{-1}$). The atmospheric pressure ranged from 936 hPa to 1034 hPa, with a mean of $992 \pm 13 \text{ hPa}$. Table SI - Supplementary Material shows the

mean annual air temperature ($^{\circ}\text{C}$), atmospheric pressure (hPa), and wind speed (m s^{-1}) measured during the 1997-2003 period in Joinville Island.

Acquisition of Sea Ice Database

Monthly data on sea ice extent and area were obtained for the period from January 1993 to November 2005, corresponding to the timeframe established through the dating of core TG1. The sea ice extent and area data from the Weddell and Amundsen-Bellingshausen Seas analyzed in this study were selected based on the geographical location of Joinville Island, where samples were collected. This database was compiled from readings taken by the Nimbus 7 Scanning Multichannel Microwave Radiometer (SMMR) satellite and the Defense Meteorological Satellite Program Special Sensor Microwave Imagers (SSM/I), and were compiled from the following web addresses: http://polynya.gsfc.nasa.gov/datasets/Spfiles_27yrs_78-05_mon.area.txt for area data and http://polynya.gsfc.nasa.gov/datasets/Spfiles_27yrs_78-05_mon.ext.txt for Antarctic Sea ice extent data.

For correlation analyses using the sea ice area separated by sectors of the Weddell and Amundsen-Bellingshausen Seas, monthly raster images from the period 1993-2005 were used. These images were acquired from the National Snow and Ice Data Center (NSIDC) website: https://nsidc.org/data/seaice_index. After acquiring the images in 24-bit bitmap format, they were exported to the IDRISI 32 program, where they were converted to 8-bit bitmap, processed to remove unwanted information, and reclassified. Reclassification was performed to differentiate between continent areas (Antarctic and South American) and islands (Joinville, South Shetland, among others) from the sea ice areas of the Weddell and Amundsen-Bellingshausen Seas. Values of zero (0) and one

(1) were assigned, respectively, to the parameters in question.

In the IDRISI 32 program, a standard geometric image was created to be used as a “mask” over all raster images. Initially, the geographical location of the island was chosen as the central point for positioning the mask. The mask’s shape was chosen so that the entire sea ice area near Joinville Island was considered during the analysis. A geometric figure in the form of four concentric circles, each with a radius of 390 km, was created. Finally, this figure was divided into four sectors named: Weddell Sea, containing Weddell South (WS) and Weddell North (WN); and, Amundsen-Bellinghshausen Seas (ABS), with Amundsen-Bellinghshausen South (BS), and Amundsen-Bellinghshausen North (BN). Uncertainties in satelital sea ice areas of this study are provided by NSIDC. The NSIDC database estimate error based on accepted knowledge of the sensor capabilities and analysis of the amount of “noise,” or daily variations not explained by changes in weather variables. For average relative error, or error relative to other years, the error is approximately 20,000 to 30,000 km², that is a small fraction of the total existing sea ice. Besides the uncertainties in the sea ice area report by NSIDC, error due to image conversion to be accessed by the IDRISI 32, processing and reclassification before using the data, also add error to sea ice area. In Figure S1 - Supplementary Material we present sea ice data output and correlations between NSIDC sea ice area and processed images (pixels) for Weddell Sea, Amundsen- Bellinghshausen Seas and Antarctica continent.

Statistical analyses

For each cation/anion dataset analyzed we applied the Shapiro–Wilk test to investigate whether or not the datasets are normally distributed (Shapiro & Wilk 1965). Taking into

account the relatively small sample sizes (ranging from 34 samples for TG2 core to 67 samples for TG2 core) the normality test is appropriate (Mishra et al. 2019). The Shapiro–Wilk test (W-statistic) is basically a measure of how well the ordered and standardized sample quantiles fit the standard normal quantiles. The W-statistic takes a value between 0 and 1 with 1 being a perfect match. For this test, null hypothesis states that data are taken from normal distributed population. Herein we assume that when $p > 0.05$, null hypothesis is accepted and data fits to normal distribution.

From the above, we found that ionic compositions from TG1 were all non-normally distributed. However, for TG2, 7 ions out of 10 presented $W > 0.7$ and were normally distributed. Although normal and non-normal distributions were found for our ionic datasets, annual averages taken from these ions concentrations were all normally distributed. Due to this fact, we have only used r-Pearson correlations with sea ice datasets.

We applied a hierarchical clustering analysis to the ionic dataset. In this case the Ward’s method with Euclidean distance (Hammer & Harper 2001). Outputs of this analysis are dendrograms that group components and may help identify associations among the glaciochemical compositions of the snow/firn. The cluster analysis was performed by PAST (Paleontological statistics) software version 4.03. The Ward’s method is a classical robust algorithm that is based on analysis of variance to evaluate the distances between groups of data, attempting to minimize the sum of the squared deviations from the cluster centroid that is created at each step of the method. The method or rule of connection between clusters (*amalgamation rule*) used in this study is that of minimum variances, or Ward’s method, with Euclidean distance, as the connection distance

(Digby & Kempton 2012). Ward is the method considered as most efficient in geophysical studies and uses a more robust algorithm based on analysis of variance to evaluate the distances between groups of data, trying to minimize the sum of the squared deviations from the cluster mean that is created at each step of the method.

RESULTS AND DISCUSSIONS

The Meteorological Data

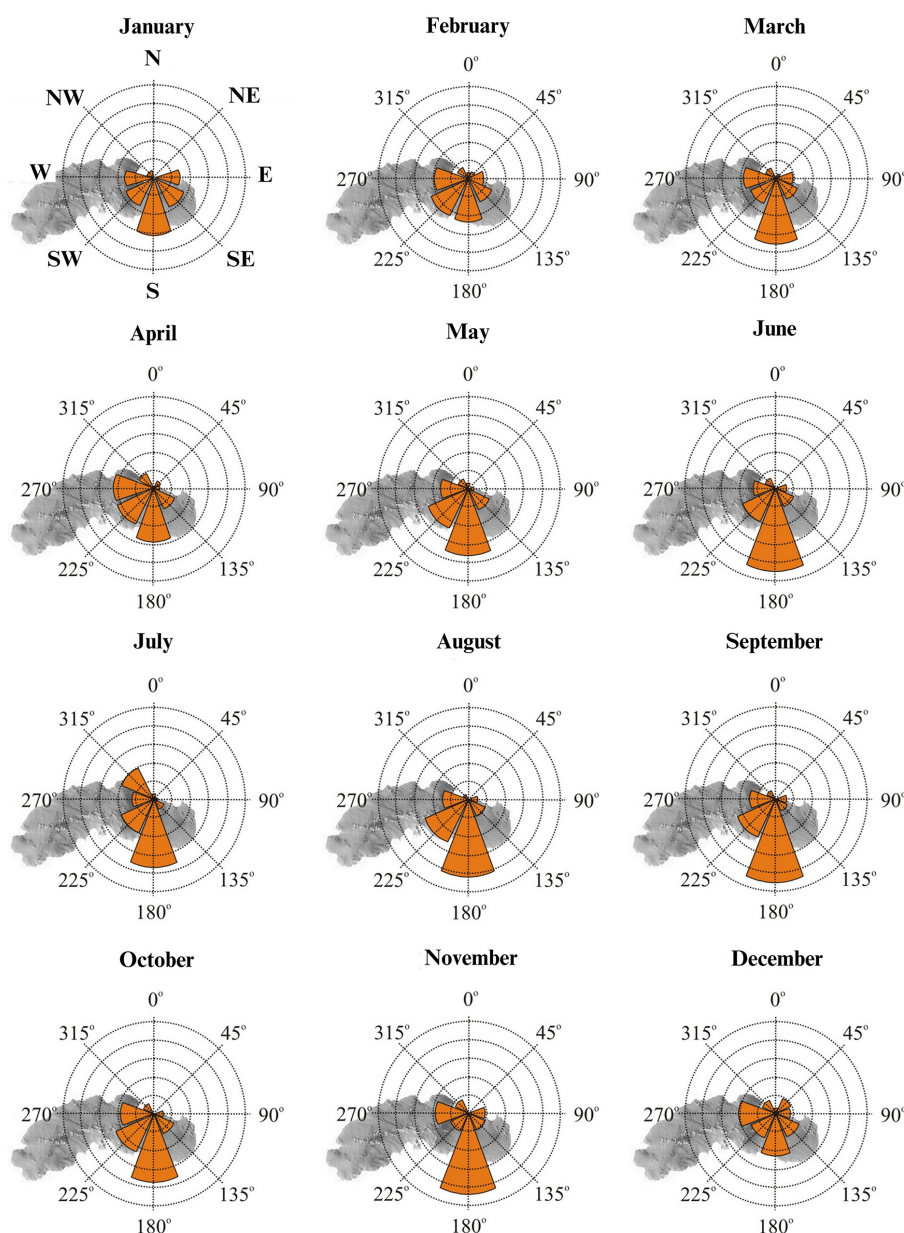


Figure 2. Monthly means of wind frequency (%) and wind direction (blowing from) measured by the automatic weather station installed on Joinville Island from 1997 to 2003. The center of the wind rose is located at the geographical point of the station. Each concentric circle represents a 10% interval.

Figure 2 presents the monthly means of wind frequency (%) and direction measured on Joinville Island from 1997 to 2003.

As observed in Figure 2, during the studied period, the main synoptic influence on Joinville Island is attributed to the meridional component, which originates from the Weddell Sea and blows towards the Bransfield Strait, primarily reaching the Island from the south sector (180°). Winds from this direction are predominant throughout the year, approximately 36%, although this

contribution varies throughout the year. There is an increase in wind intensity in May and a decrease in November, corresponding to the Austral winter.

Winds from the southwest sector (225°) also occurred with relatively high frequency (20%). Winds from the west (270°), southeast (135°), northwest (315°), and east (90°) sectors contributed 16%, 12%, 7%, and 6% of the total annual wind reaching the Island, respectively. The lowest wind frequency contributions observed in this location were from the north (1%) and northeast (2%) sectors.

The higher frequency of winds reaching the south sector of Joinville Island can be explained by its geographical location. The Island is influenced by inertial winds, which are cold and strong, coming from the Weddell Sea. As these winds travel towards the South Shetland Islands, they pass between Joinville Island and the Antarctic Peninsula, causing a decrease in local temperature (Meredith & King 2005, Trusel et al. 2013). The high frequencies of winds reaching the southwest (20%) and west (16%) sectors of the Island may be related to katabatic winds originating from the northern end of the Antarctic Peninsula (Parish & Cassano 2003).

The Joinville is off the northern Antarctic Peninsula region and exhibits glaciological and climatic characteristics distinct from those in the continental Antarctic region. Therefore, a significant portion of the results obtained in this study is better compared with findings from studies conducted in the Antarctic Peninsula area, particularly those reported for King George Island (KGI, 62°S - 58°W) and James Ross Island (JRI, 64°S - 57°W).

Ionic concentrations, dating, and stratigraphy of snow/firn core

Figures 3 and 4 show the depth variation (cm and cm water equivalent) of the concentrations (ng g^{-1} and $\mu\text{Eq L}^{-1}$) of cations and anions in cores TG1 and TG2, respectively.

The comparison of the depth concentration variation graphs showed that, in general, there is a considerable difference between cores TG1 and TG2. This difference may be associated with local melting patterns, conditioned by temperature variations at the two sampling points with an altitude difference of 112 m.

In both cores, TG1 and TG2, a marked similarity can be observed in concentration patterns between Cl^- and Na^+ ions and between Mg^{2+} and SO_4^{2-} , reflecting their oceanic origin. In general, chemical compounds found deposited in snow and ice samples from Antarctic regions are transported through the atmosphere by primary aerosols (sea salt and continental dust) and secondary aerosols (produced through gas emissions from biogenic and/or anthropogenic sources) (McConnell et al. 2007, Wolff et al. 2010).

Specifically, the behavior of the MSA anion in core TG2 indicates that this site suffers intense vertical percolation (Figure 4g). So, the MSA variability is also a consequence of post-depositional processes (melting, percolation, and refreezing) common in the Antarctic Peninsula, where air temperatures can reach positive values even during winter.

The melting of snow and firn core results in the preferential elution of some ions relative to others, and this phenomenon occurs due to their physicochemical differences (Grannas et al. 2007). Several studies have indicated that MSA is highly susceptible to modifications resulting from post-depositional processes, which would lead to a loss of the initial signal and, consequently, an alteration in the seasonal pattern of its deposition (Legrand & Pasteur 1998, Jiankang et al. 2001). In core TG1, MSA, originating from marine biological activity, appears not to

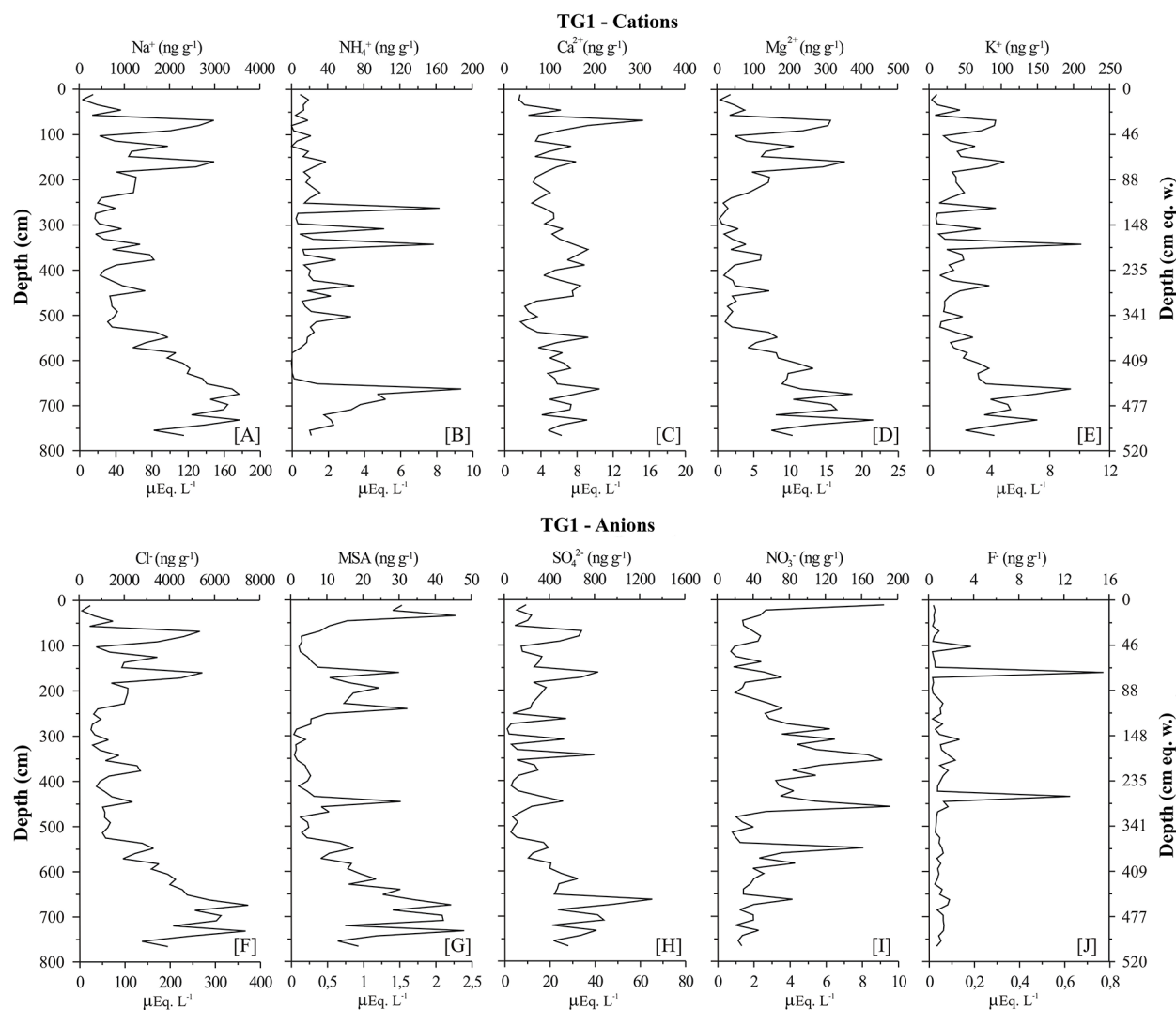


Figure 3. Variation of concentration (ng g^{-1} and $\mu\text{Eq L}^{-1}$) with depth in the TG1 core for cations: [A] = sodium (Na^+), [B] = ammonium (NH_4^+), [C] = calcium (Ca^{2+}), [D] = magnesium (Mg^{2+}), [E] = potassium (K^+), and anions: [F] = chloride (Cl^-), [G] = methanesulfonic acid (MSA), [H] = sulfate (SO_4^{2-}), [I] = nitrate (NO_3^-), [J] = fluoride (F^-).

have undergone the same processes observed in TG2, thus exhibiting a depth variation similar to that of oceanic ions Cl^- , Na^+ , and Mg^{2+} .

The dating of the TG1 snow/firn was done by examining the seasonal variations in d^{18}O and the ionic species Na^+ and SO_4^{2-} (Figure 5). The TG2 core was not dated due to the intense melting, percolation, and refreezing, damping the original seasonal variations.

The d^{18}O data in core TG1 showed a mean of $-11.53 \pm 1.96\text{‰}$, with a minimum and maximum of -19.39‰ and -7.30‰ , respectively. This mean

value is very close to values reported by other authors for the Antarctic Peninsula region (Ming 1997, Simões et al. 2004).

Global volcanic eruption records are commonly used as reference horizons (Vinther et al. 2006, Sigl et al. 2014) for dating snow and ice cores. Eruptions such as Pinatubo, in 1991, released large volumes of SO_4^{2-} , gases (H_2S , SO_2), dust, and crustal material directly into the stratosphere (Dixon et al. 2005). Additionally, glaciological studies in the Antarctic Peninsula region can use records of eruptions in Deception

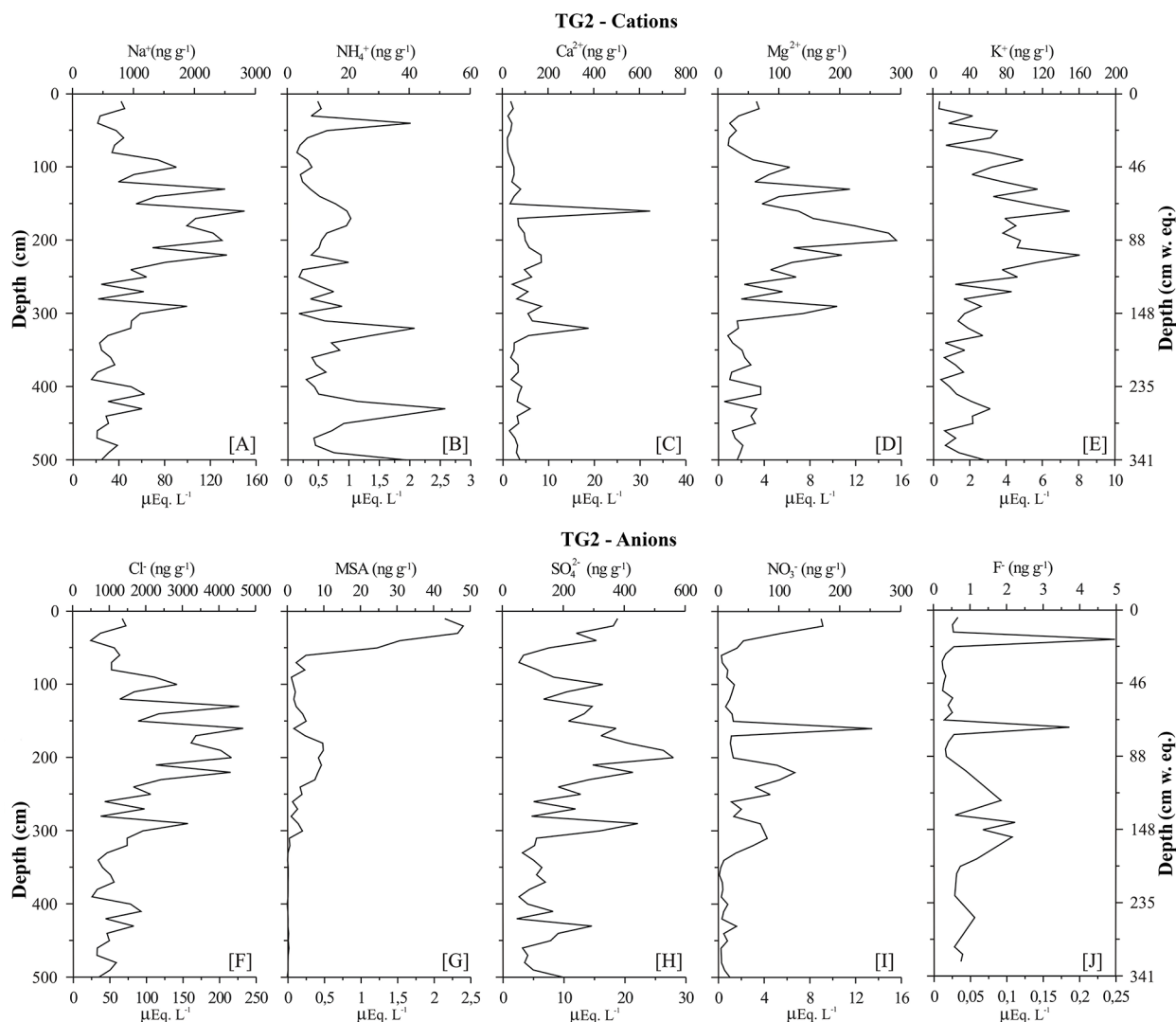


Figure 4. Variation of concentration (ng g^{-1} and $\mu\text{Eq L}^{-1}$) with depth in TG2 core for cations: [A] = sodium (Na^+), [B] = ammonium (NH_4^+), [C] = calcium (Ca^{2+}), [D] = magnesium (Mg^{2+}), [E] = potassium (K^+), and anions: [F] = chloride (Cl^-), [G] = methanesulfonic acid (MSA), [H] = sulfate (SO_4^{2-}), [I] = nitrate (NO_3^-), [J] = fluoride (F^-).

Island, located in the South Shetland Islands (Aristarain & Delmas 2002).

Several ice lenses and layers of varying thicknesses were found in the core sections. Most of them were within seven discontinuous zones, as shown in Figure 6 (indicating that the TG1 core is intercalating snow/firn layers with refrozen ice layers). No layers containing high concentrations of microparticles (e.g. volcanic ashes) were observed, indicating that the core was not long enough to reach the snow layers

where regional-scale volcanic eruption records were deposited.

From the surface to a depth of 200 cm (88 cm w.eq.), a marked transition in the type of snow found in the core was observed. Initially, a layer of fresh snow was observed, followed by layers of snow with grains smaller than 3 mm, becoming larger than this at the bottom.

A depth hoar layer was identified at a depth of 155 cm (70 cm w.eq.), indicated as Dh in Figure 6. This kind of layer with a low density (in this case, 0.3 g cm^{-3}) is formed when there is a

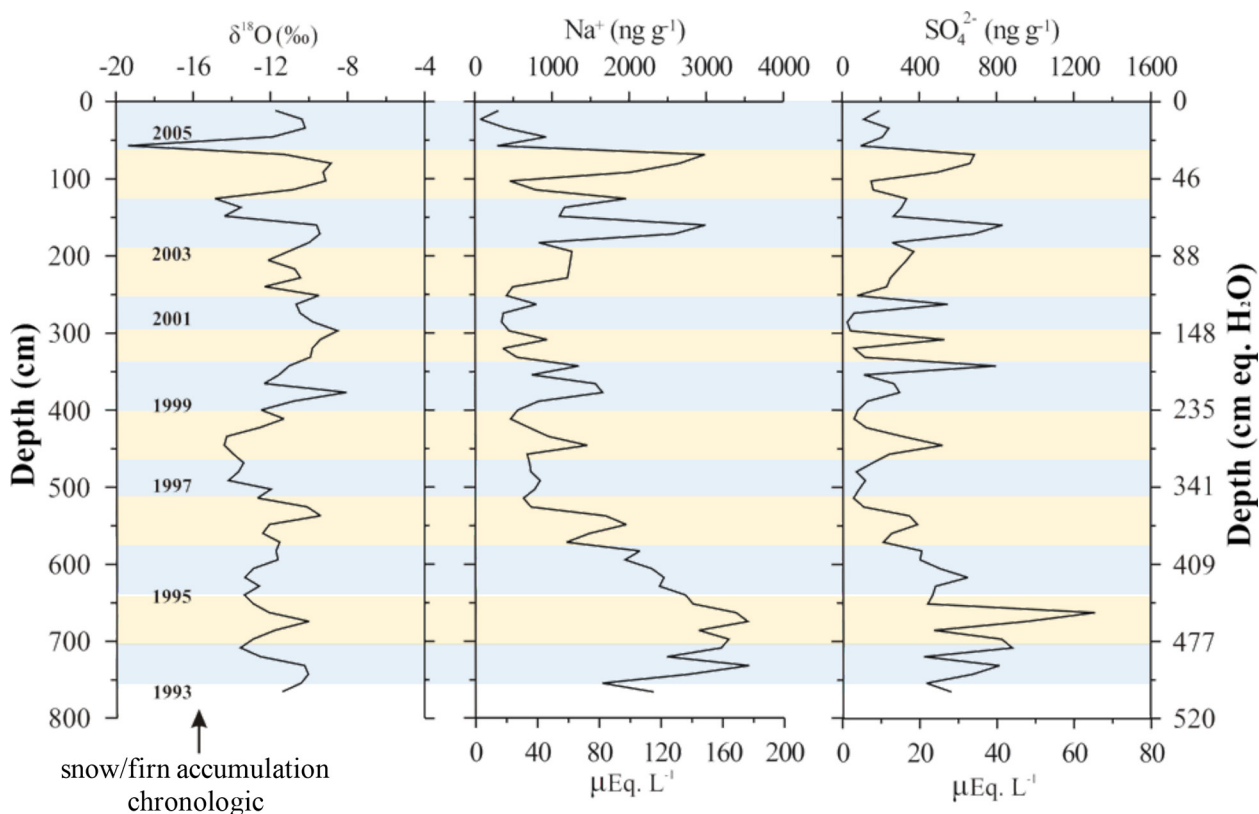


Figure 5. Depth variation (cm w. eq.) of $d^{18}\text{O}$ (in ‰), Na^+ , and SO_4^{2-} (ng g^{-1} and $\mu\text{Eq L}^{-1}$) in snow/firn core TG1 from Joinville Island through the years (years ± 2).

marked vertical temperature difference between two unconsolidated snow layers, which creates a strong vapor pressure gradient. The snow sublimates and recrystallizes.

The highest concentrations of ice layers are 360 cm (194 cm w.eq.) and 550 cm (375 cm w.eq.) deep, associated with the 2000 to 1998 precipitation years, respectively. This high number of ice layers is related to intense melting processes caused by high temperatures observed on Joinville Island during those years.

The statistics of ions in TG1 and TG2

The statistical method applied for cations and anions measured are showed in Table I.

Table I shows difference between the majority of the analyzed elements in the two cores, indicating that TG1 and TG2, despite suffering similar processes of dry or wet deposition

(snow or rain) as they are separated by only 1.5 km, are subject to different post-depositional processes (melting, percolation, refreezing). On the other hand, the altitude difference between the two (112 m) is sufficient to maintain TG1 more preserved than TG2, restring post-depositional processes that may alter the ionic composition of the deposits.

In both cores, the Na^+ and Cl^- ions exhibited the highest mean concentration among the analyzed ions. These two elements together contribute the largest portion of the total ions deposited in Joinville Island, accounting for 88% in TG1 and 85% in TG2. These values agree with the findings of Legrand & Mayewski (1997), who proposed that sea salt contributes to approximately 85% of the impurities found in coastal Antarctic regions.

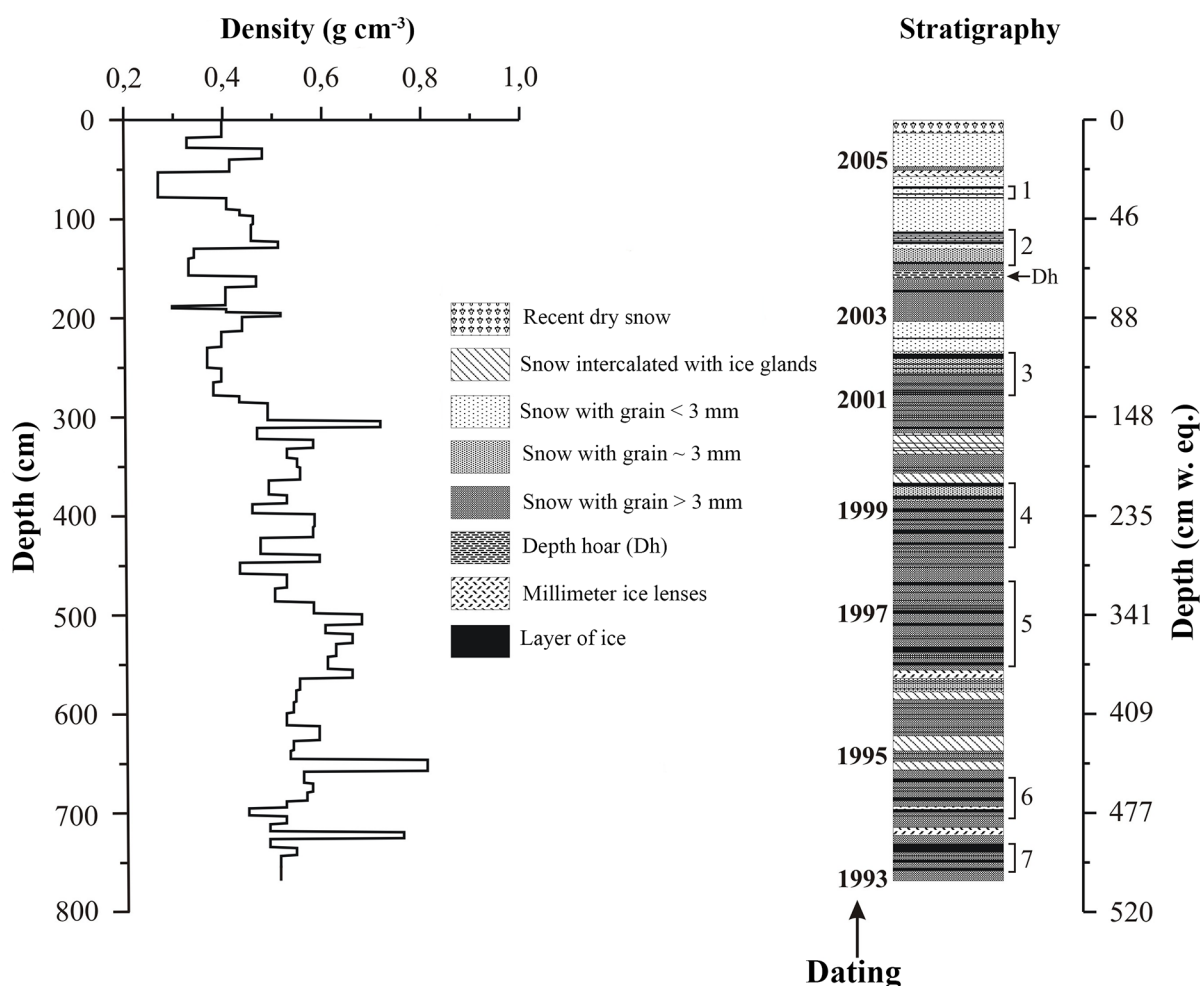


Figure 6. Density profile (g cm^{-3}) and stratigraphy along the 800 cm depth (490 cm w.eq.) of core TG1. The numbers (1-7) on the right side of the stratigraphy represent zones with high concentrations of ice layers. "Dh" indicates the location of the depth hoar layer, and the core dating is presented to the left of the stratigraphy.

At KGI, Jiahong et al. (1998) demonstrated that these elements contribute to 84% of the total ionic concentration, while Simões et al. (2004) found high concentration values for Cl^- and SO_4^{2-} . According to these authors, the high relative concentration of these elements in KGI can be attributed to characteristics that also apply to Joinville Island: (1) the low altitude of the core sampling site (566 m above sea level) and (2) sampling point relatively close to the sea (~6 km distance), associated with high wind speed and intense local cyclonic activity,

favoring the formation and transport of marine aerosols.

Total glaciochemical data from Joinville cores were submitted to a hierarchical clustering analysis (Ward's method) in order to search for association among the different ions measured (Figure 7).

From Figure 7, one Group of ions and two Sub-groups were clearly evidenced from the method: Group 1: Cl^- and Na^+ ; Sub-group 2.1: Ca^{2+} , Mg^{2+} and SO_4^{2-} and; Sub-group 2.2: NO_3^- , K^+ , MSA, NH_4^+ and F^- . Both Group 1 and Sub-group 2.1 reflect the major constituents of sea spray and

Table I. Descriptive statistics of concentrations (in $\mu\text{Eq L}^{-1}$) of Na^+ , NH_4^+ , Ca^{2+} , Mg^{2+} , K^+ , Cl^- , MSA , SO_4^{2-} , NO_3^- and F^- in the TG1 and TG2 cores in Joinville Island. SD: Standard Deviation.

		Descriptive Statistics ($\mu\text{Eq L}^{-1}$)									
		F ⁻	MSA	Cl ⁻	NO ₃ ⁻	SO ₄ ²⁻	Na ⁺	NH ₄ ⁺	K ⁺	Mg ²⁺	Ca ²⁺
TG1	Shapiro-Wilk (W-statistics)	0.364	0.159	0.167	0.174	0.120	0.156	0.273	0.150	0.159	0.099
	p-value	<0.01	<0.01	<0.01	<0.01	<0.01	<0.01	<0.01	<0.01	<0.01	<0.01
	Geometric mean	0.047	0.459	94.3	2.483	13.1	56.7	0.778	2.028	4.32	5.22
	Geometric SD	2.067	2.796	2.120	1.914	2.432	2.024	4.925	2.129	2.653	1.538
	Arithmetic mean	0.069	0.724	127.4	3.084	18.09	73.93	1.572	2.744	6.504	5.821
	Arithmetic SD	0.119	0.638	93.50	2.198	13.52	49.35	1.947	2.141	5.323	2.789
	Minimum	0.016	0.044	6.348	0.762	1.370	3.698	0.001	0.182	0.336	1.654
	Maximum	0.774	2.401	374.5	9.584	65.60	177.9	9.398	10.53	21.63	16.64
	Samples (n)	65	66	66	66	66	66	65	66	66	66
TG2	Shapiro-Wilk (W-statistics)	0.637	0.555	0.846	0.707	0.919	0.859	0.804	0.931	0.821	0.533
	p-value	<0.01	<0.01	<0.01	<0.01	<0.01	<0.01	<0.01	<0.01	<0.01	<0.01
	Geometric mean	0.033	0.083	73.03	1.167	8.605	44.19	0.582	2.099	2.923	3.415
	Geometric SD	2.138	5.825	1.823	2.960	1.942	1.787	1.933	2.221	2.270	1.949
	Arithmetic mean	0.046	0.322	87.63	2.087	10.54	52.37	0.726	2.738	4.050	4.493
	Arithmetic SD	0.051	0.592	56.85	2.554	6.570	32.59	0.540	1.847	3.475	4.949
	Minimum	0.012	0.000	24.75	0.125	2.357	15.596	0.159	0.332	0.523	1.104
	Maximum	0.248	2.406	233.2	12.67	28.06	141.2	2.593	8.034	14.65	32.35
	Samples (n)	34	48	50	50	50	50	50	50	50	50

their high influence in the Maritime Antarctica boundary layer. As demonstrated above and by several other studies, Cl^- and Na^+ are overall linked to the sea ice dynamics and the local winds strengths while Ca^{2+} , Mg^{2+} and SO_4^{2-} are second order major constituents of seawater by weight (after Cl^- and Na^+). Unlike the other ions, sulphate may have other sources in Antarctic coastal areas like biogenic, from the summer

primary productivity, and from polynyas areas that are formed in sea ice and are considerable sources of salt flux, mainly in winter (Arrigo & van Dijken 2003). As mentioned before, volcanism is also an important source for sulphate in the global cryosphere. Sub-group 2.2 has a direct relation with the biogenic aerosols derived from the primary productivity. MSA is an oxidation product of DMS while for Antarctica the major

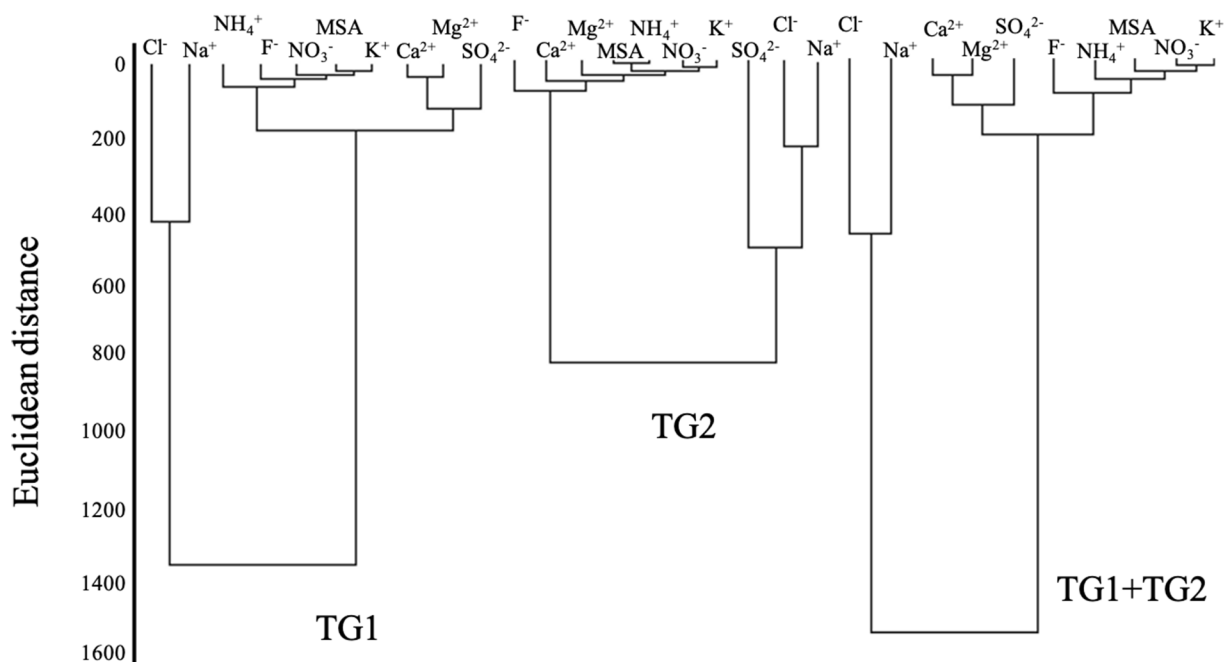


Figure 7. Dendrograms from hierarchical clustering analysis (Ward's method with Euclidean distance) using ionic datasets of cores TG1, TG2 and integrated data of TG1+TG2.

component of the NH_4^+ originates from oceanic emissions produced by diatoms (microscopic algae) from the Southern Ocean, although very little influence of long-range transport from biomass burning could also be present (Legrand et al. 2021). NO_3^- is the atmospheric precursor of NH_4^+ .

For the coastal Antarctica NO_3^- can be also emitted penguins due to degradation of urea (nitrogenous waste that comes from the degradation of proteins by the liver). In general seawater NH_x originates from the degradation of organic matter or nitrogen fixation from the water surface and serves as a nutrition source for phytoplankton (Legrand et al. 1998). The origin of fluoride in ice core is still uncertain. For the Southern Ocean, it is found high concentrations of fluoride in the body parts of several crustaceans from a variety of marine habits, especially in the exoskeleton of *Euphausia superba* and *Euphausia crystallorophias* (Sands et al. 1998), which is abundant in the

Weddell Sea around the Joinville Island. On the other hand, abrupt increases observed in our database may also point for a possible long-range atmospheric transport associated with volcanism as suggested by Severi et al. (2014) by several snow pits from the route Northern Victoria Land to Dome C route, in the framework of the ITASE (International Trans-Antarctic Scientific Expedition) program.

Use of $\text{Mg}^{2+}/\text{Na}^+$ ratio for Melting Investigation

Iizuka et al. (2002) proposed, from empirical observations, that the use of the $\text{Mg}^{2+}/\text{Na}^+$ ratio behaves as a good indicator of seasonal melting. They compared $\text{Mg}^{2+}/\text{Na}^+$ ratios of dry and wet snow/firn samples from sectors of several cores obtained in the Arctic region. According to these authors, the lower the ratio value in relation to 0.12, the more intense the melting process would be. The authors attribute that to differential ion-flushing processes during melting and percolation in which Mg^{2+} and Na^+ are individually

submitted after surface deposition. From Figure 8 one may observe that TG1 ratios have more data closer to 0.12 value than TG2. This suggest that despite possible melting affecting both ice cores, TG1 better preserve its natural conditions.

Correlation Between Glaciochemistry and Sea Ice

In search examination of a consistent proxy for sea ice variability in the northern Antarctic Peninsula region, we compared the mean annual ionic concentrations in core TG1 with the measured and calculated wind speed, the sea ice extent and area in the Amundsen-Bellinghshausen and Weddell Sea. For wind speed, the data used were from the Argentinian Esperanza weather station (63°24' S, 56°59' W), the closest weather station to sampling point.

The sea ice database acquisition was done using satellite data, and the selection of Na^+ , Cl^- , and MSA for comparison was based on studies that demonstrated they serve as proxies for sea ice variability (e.g. Abram et al. 2013, 2011, Curran et al. 2003, Thomas et al. 2019)

During the period of this study (1993–2005), the mean annual sea ice extent for the Weddell Sea was $42.3 \pm 2.3 \times 10^5 \text{ km}^2$, while the Amundsen-Bellinghshausen Seas (ABS) showed a value of $13.9 \pm 0.6 \times 10^5 \text{ km}^2$. The annual mean sea ice area in the Weddell and ABS had values of $33.7 \pm 1.9 \times 10^5 \text{ km}^2$ and $9.9 \pm 0.5 \times 10^5 \text{ km}^2$, respectively. The Pearson correlation coefficients (r) between the Na^+ , Cl^- , MSA elements measured, sea ice parameters, and local wind speed values for the ions from core TG1 used in this correlation

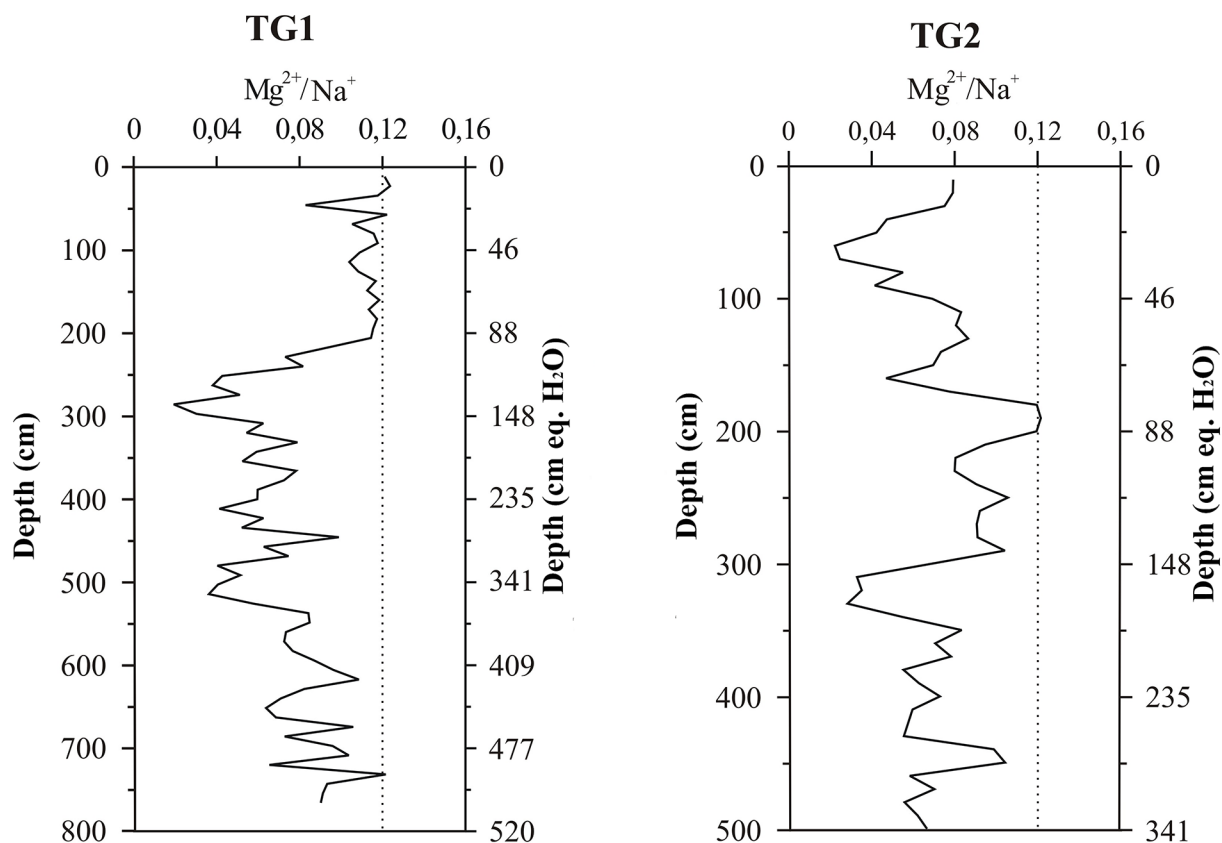


Figure 8. Vertical distribution of the $\text{Mg}^{2+}/\text{Na}^+$ ratio in cores TG1 and TG2 from Joinville Island. The dotted line indicates the mean value of this ratio in seawater (0.12).

analysis are presented in Table II. The mean annual wind speed on Joinville Island (measured and calculated) between 1993 and 2005 was $10.4 \pm 1.05 \text{ m s}^{-1}$.

In the database of both ice cores, the ionic composition of Na^+ and Cl^- presented same correlation levels between them (Pearson's $r = 0.94$, $\alpha < 0.05$, $n = 66$ and 50 , respectively) (Figure 3 and 4). Despite the several reports on post-depositional chemical processes taking part in the snowpack effecting Cl^- concentrations (e.g. Legrand & Delmas 1988), in the case of Joinville Island it does not seem to be a problem and both ions were used for sea ice correlations. The significant correlation value between these elements reflect that they have the same origin, seawater spray, and indicates that core TG1 is well preserved. Meanwhile, their correlations ($r = 0.67$ and $r = 0.83$, respectively) with MSA suggest that these three ions may be subject to the same local transport mechanisms.

Analyzing the correlation values of the sea salt elements with MSA separately, a better correlation is observed with Cl^- . This result may be related to the fact that MSA is also an anion,

like Cl^- ; therefore, it is subject to more similar deposition processes when compared to Na^+ . On the other hand, the strong correlations of sea ice extent and area, both for the Weddell Sea ($r = 0.93$) and the ABS ($r = 0.94$), were expected since these are different ways for the satellite to analyze the same environmental parameter (sea ice).

In a recent work by CLIVASH2k (CLimate Variability in Antarctica and the Southern Hemisphere over the past 2000 years) working group (Thomas et al. 2023) a comprehensive Na^+ database study was performed on Antarctic ice cores. They mapped sites where Na^+ correlated with the corresponding sea ice concentrations, geopotential height (500 hPa), the surface wind strength and atmospheric circulation. They reported that Na^+ at several places of Antarctica, mostly at the West Antarctica, do respond to wind strength. From this finding, we decided also to investigate the relations of Na^+ with this meteorological parameter for Joinville Island. Two aspects were determined from our work: a) wind and Na^+ do correlate, at the annual base, as shown in Figure 9. However, we also observe that

Table II. Pearson correlation coefficients (r) between the Na^+ , Cl^- , MSA elements measured in core TG1, sea ice parameters, and local wind speed, where: W (Weddell Sea), ABS (Amundsen-Bellinghshausen Seas), ext. (sea ice extent), area (sea ice area), WS Joinv. (wind speed on Joinville Island). The values in bold are statistically significant (t-Student test) for $\alpha = 0.05$ and $n = 13$.

	Na^+	Cl^-	MSA	W ext.	ABS ext.	W area	ABS area	WS Joinv.
Na^+	1							
Cl^-	0.94	1						
MSA	0.67	0.83	1					
W ext.	0.42	0.46	0.54	1				
ABS ext.	0.36	0.39	0.21	0.15	1			
W area	0.27	0.37	0.51	0.93	0.24	1		
ABS area	0.44	0.46	0.30	0.23	0.94	0.26	1	
WS Joinv.	0.59	0.51	0.12	0.05	0.44	-0.01	0.31	1

most important changes in Na^+ are not captured by the wind dataset; b) while integrating the sea ice at Weddell Sea and Amundsen-Bellingshausen sub-sectors, correlations with MSA, Na^+ and Cl^- are considerably higher, as shown in Figure 11. In summary, at Joinville Island Na^+ correlates with both surface wind and sea ice extent. In addition, Na^+ correlations with sea ice are significantly higher and can provide the total geographical extent where both parameters are related.

Comparison of the concentrations of Na^+ and Cl^- ions deposited in the TG1 core did not show a statistically significant correlation (see Table II) with the total sea ice data (extent and area) for the Weddell and ABS during the analyzed period (1993-2005). On the other hand, the annual mean concentration of MSA shows a statistically significant correlation (95% confidence; $n = 13$) with the extent ($r = 0.54$) as well as the area ($r = 0.51$) of sea ice in the Weddell Sea.

For several Antarctic sectors, as Victoria Land and Law Dome, positive correlations were found between MSA and sea ice extent (Welch et al. 1993, Curran et al. 2003). In the Southern Ocean, DMS producing organisms (precursors to MSA) are predominantly represented by marine algae, whose activity generates large quantities of DMS in areas with decreased sea ice cover during the summer (Curran et al. 2003). However, the detailed mechanism of this relationship is quite complex, as several factors may interfere with this relationship depending on the analyzed region. By applying the ice separation methodology by sectors, adapted from Curran et al. (2003), it was possible to analyze the sea ice areas of the Weddell and ABS divided into North and South sectors (BN and BS) and further divided into sub-sectors (1, 2, 3, and 4), as proposed below at item 2.5. The result of the correlation between the annual mean sea ice area (km^2) in the sub-sectors and the

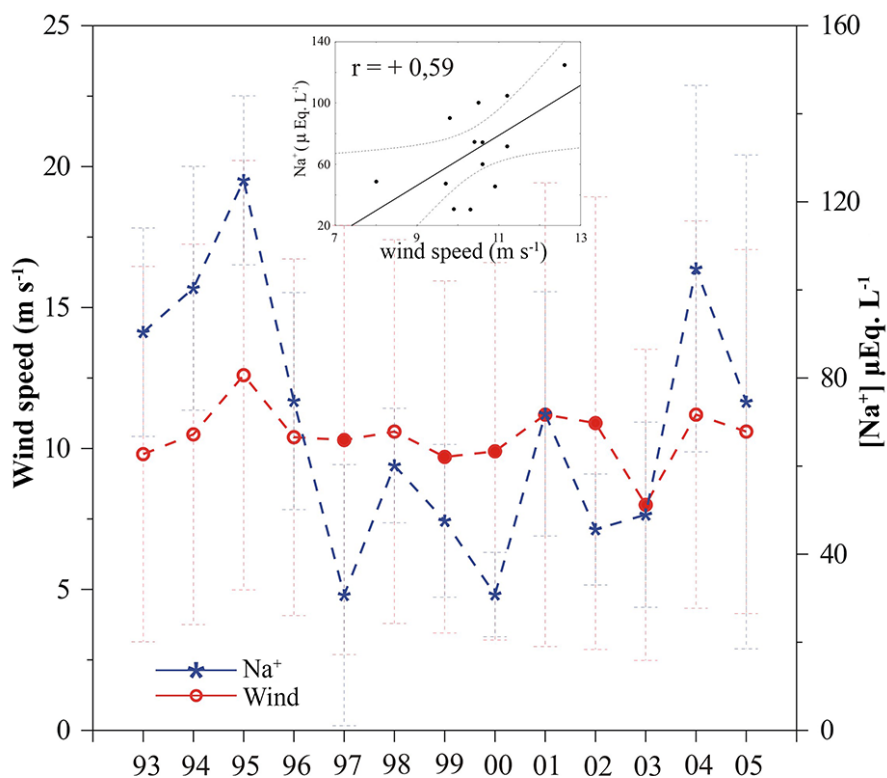


Figure 9. Variation of the annual mean concentration of Na^+ ($\mu\text{Eq L}^{-1}$) in TG1 and wind speed (m s^{-1}), measured (open circle) and calculated (closed circle) for Joinville Island in the 1993-2005 period. The dotted horizontal bars represent the standard deviation of each mean value. The smaller graph shows the correlation between the two parameters, highlighting Pearson's r value ($\alpha < 0.05$, $n = 13$).

concentration of MSA deposited in the core from Joinville Island is shown in Figure 10.

Figure 10a shows that sub-sector 3 of the WS shows the strongest correlation of the mean sea ice area with the MSA concentration in the Joinville Island (TG1 core). The significant correlation ($r = 0.78$) indicates that this sub-sector of the Weddell Sea strongly influenced the MSA concentrations deposited on Joinville Island during the analyzed period (1993–2005).

These winds are believed to be the primary drivers of MSA transport from the Weddell Sea to the Joinville Island ice cap. The observed strong correlations between the MSA and the sea ice area in sectors and sub-sectors of the Weddell and ABS led us to investigate further

their relationships with the seawater contents (Na^+ and Cl^-), which are used as a proxy of this environmental parameter. Initially, these elements did not show statistically significant correlations compared to the total sea ice data from satellite analyses (see Table II).

The results of this correlation analysis between the annual mean concentrations of Na^+ and Cl^- ($\mu\text{Eq L}^{-1}$) with the mean annual sea ice area in the sub-sectors of the Weddell and ABS are shown in Figure 11.

From Figure 11, it is clear that these new correlations of the MSA content with sea ice areas exhibited higher values (Pearson's r) than the initial ones (which used "raw" satellite data of sea ice area and extent). Similar to the

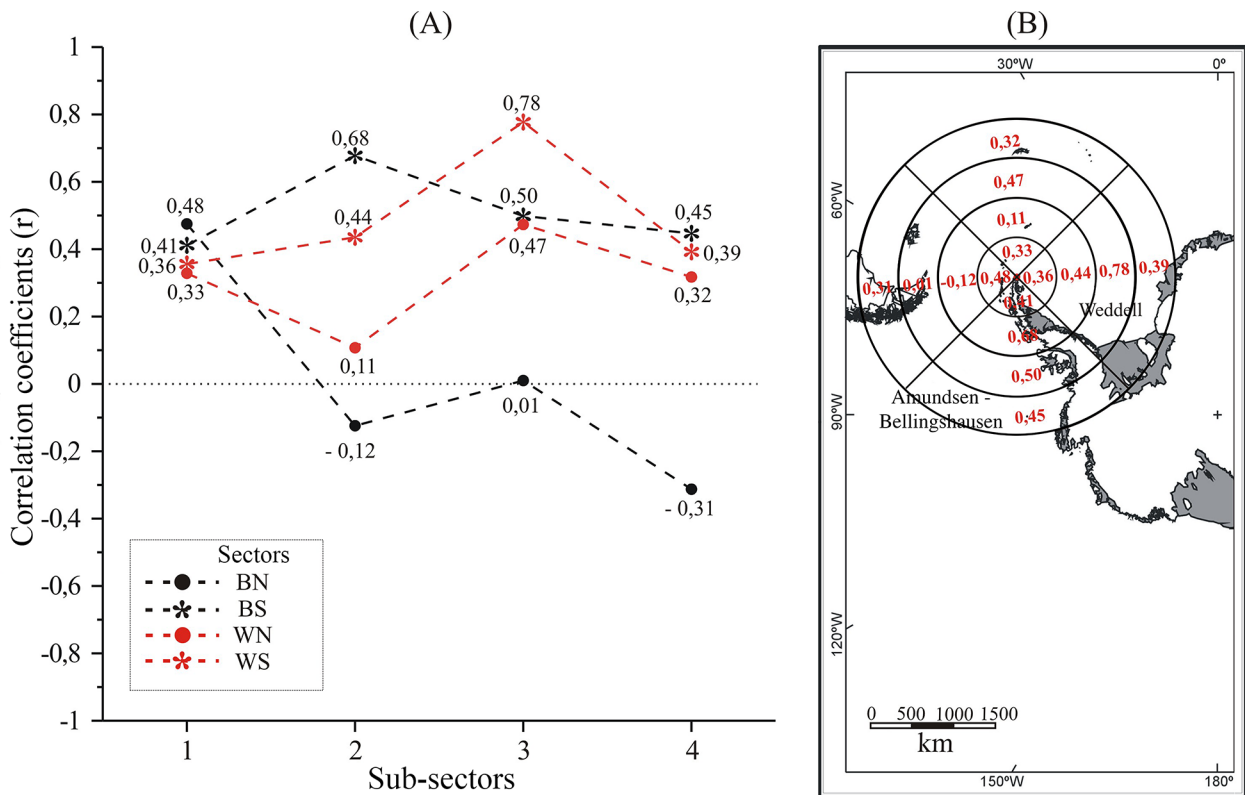


Figure 10. a) Correlation coefficients (Pearson's r , $\alpha < 0.05$, $n = 13$) of the annual mean sea ice area (km^2) in the Weddell Sea (North Weddell sector (WN) and South Weddell sector (WS) versus the concentration of MSA ($\mu\text{Eq L}^{-1}$) in the Joinville Island core. The sub-sectors are identified on the x-axis as 1, 2, 3, and 4. **b)** Partial map of Antarctica showing the correlation coefficients distribution in the mask established for this analysis (corresponding to the 1993–2005 period).

correlation analysis with MSA, Na⁺, and Cl⁻ showed the highest correlation values compared to the annual mean sea ice area in the WSS sector, sub-sector 3 (WS3), respectively, r = 0.59 and r = 0.66. Demonstrating once again the significant influence of winds from the South sector, the primary driver of transporting these elements produced in the Weddell Sea region.

Analyzing each ion separately (Na⁺ and Cl⁻), differences can be observed in the correlation values (Pearson's r) for same radial distance, depending on the sector. In the case of Figure

11a it shows that sea ice correlations with Na⁺ exhibited significance only in three cases (t-Student test, α = 0.05 and n = 13), two of these with the South Weddell sectors (WS2: r = 0.51 and WS3: r = 0.59) and one in the North Weddell sector (WN3: r = 0.53). For Cl⁻ five statistically significant positive values were found, one in the South Weddell sector (WS3: r = 0.66), one in the North Weddell sector (WN3: r = 0.53), and three in the South Amundsen-Bellingshausen sector (BS2: r = 0.58, BS3: r = 0.52, and BS4: r = 0.51) (Figure 11b).

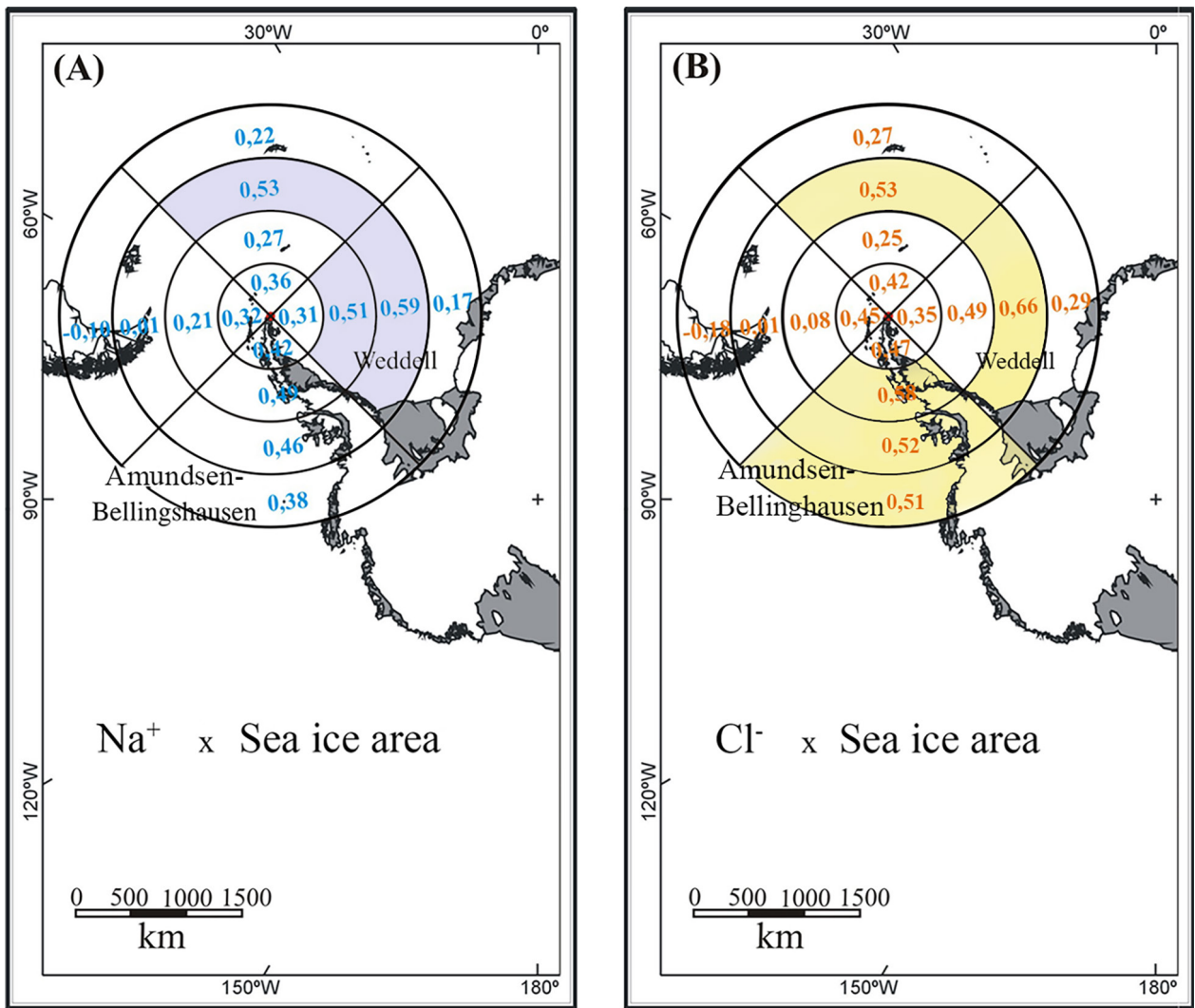


Figure 11. Correlation coefficients (Pearson's r, α < 0.05, n = 13) of the annual mean sea ice area (km²) in the Weddell and Amundsen-Bellingshausen sub-sectors versus the concentration of Na⁺ (μEq L⁻¹) in (a) and Cl⁻ (μEq L⁻¹) in (b) in the core from Joinville Island for the period 1993 to 2005. The sectors with statistical significance were highlighted.

Additionally, a correlation analysis was conducted between the concentration data of MSA, Na⁺, and Cl⁻ measured on Joinville Island and the sum of the annual mean sea ice area in the following sectors: South Weddell (WS1, WS2, WS3, and WS4), North Weddell (WN1, WN2, WN3, and WN4), and South Amundsen-Bellingshausen (BS1, BS2, BS3, and BS4), as shown in Table III. The North Amundsen-Bellingshausen sector (BN) was not included in this analysis as it exhibited the lowest sea ice concentrations during the analyzed period (1993-2005), consequently resulting in the lowest correlation values (Figures 9 and 10).

It can be noticed in Table III that among the summation configurations of annual mean sea ice from the WS sub-sectors the configuration represented by WS1, WS2, and WS3 showed the

strongest correlations with MSA ($r = 0.75$), Na⁺ ($r = 0.63$), and Cl⁻ ($r = 0.68$). However, when observing the correlation values of these elements with the summations of sea ice from the WN + WS, only the configuration represented by the summation of WN3 + WS3 showed statistically significant correlations with the ions in question (MSA: $r = 0.74$, Na⁺: $r = 0.64$, Cl⁻: $r = 0.69$). This indicates that the WN sector has little influence on the MSA deposited on Joinville Island and can be excluded from future analyses.

Instead, the summation configurations between the WS+BS showed the highest statistically significant correlations. The WS2+BS2 arrangement showed the highest correlation values with MSA ($r = 0.77$), Na⁺ ($r = 0.64$), and Cl⁻ ($r = 0.71$), indicating that the BS sector also suffers

Table III. Correlation coefficients (Pearson's r) between the concentrations of MSA, Na⁺, and Cl⁻ ($\mu\text{Eq L}^{-1}$) in the core from Joinville Island and the sum of the annual means of sea ice area in sub-sectors (1, 2, 3, and 4) of the Weddell (North - W.N., and South - W.S.) and Amundsen-Bellingshausen (South - B.S.) seas. The values in bold are statistically significant at $\alpha = 0.05$ and $n = 13$ (t-Student test).

	MSA	Na ⁺	Cl ⁻
<i>Sum of sub-sectors</i>	<i>r-Pearson</i>		
<i>Inside the WS sector</i>			
WS1+WS2	0.43	0.46	0.47
WS1+WS2+WS3	0.75	0.63	0.68
WS1+WS2+WS3+WS4	0.70	0.53	0.61
<i>WN + WS</i>			
WN1+WS1	0.38	0.38	0.43
WN2+WS2	0.25	0.38	0.36
WN3+WS3	0.74	0.64	0.69
WN4+WS4	0.45	0.24	0.36
<i>WS + BS</i>			
WS1+BS1	0.59	0.55	0.62
WS2+BS2	0.77	0.64	0.71
WS3+BS3	0.73	0.59	0.66
WS4+BS4	0.45	0.27	0.41

a strong influence on the concentration of these elements deposited on Joinville Island.

So, the strong influence of the sea ice area from both the WS and BS sectors, another correlation analysis was performed with the outline of all arrangements (WS+BS) that showed statistically significant correlation values. The summary of these sub-sectors (WS1+WS2+WS3+BS1+BS2+BS3) proved to be the best configuration among the previously analyzed ones, as it exhibited the highest correlation values with the analyzed elements: MSA ($r = 0.80$), Na^+ ($r = 0.66$), and Cl^- ($r = 0.74$).

Figure 12 compares variations in the mean annual concentrations of MSA, Na^+ , and Cl^- ($\mu\text{Eq L}^{-1}$), with the mean annual sea ice area corresponding to the summation of sub-sectors WS1+WS2+WS3+BS1+BS2+BS3 (hatched area), for the period 1993–2005. The correlations between sea ice and these concentrations are also shown, highlighting Pearson's r value ($\alpha < 0.05$, $n = 13$).

The treatment of “raw” sea ice data from the Weddell and ABS allowed for identifying the area with the most significant potential to influence the concentration of MSA, Cl^- , and Na^+ elements in the Joinville Island ice cap during the p1993–2005 period. The delimitation of this area is essential to detailed analysis in the search for a consistent proxy of sea ice variability in the Antarctic Peninsula region. The sea ice database (area and extent) of the Weddell and Amundsen-Bellingshausen seas, established through satellite analyses, relates to the total area of these seas, whose boundaries are shown in Figure 12b (dotted lines).

The positive correlations between the sea salt elements (Na^+ and Cl^-) and the sea ice area differ from what was observed by Aristarain et al. (2004). These authors presented an anti-correlation between the extent of sea ice in the Weddell Sea and the concentration of Cl^- deposited in a core collected on James Ross

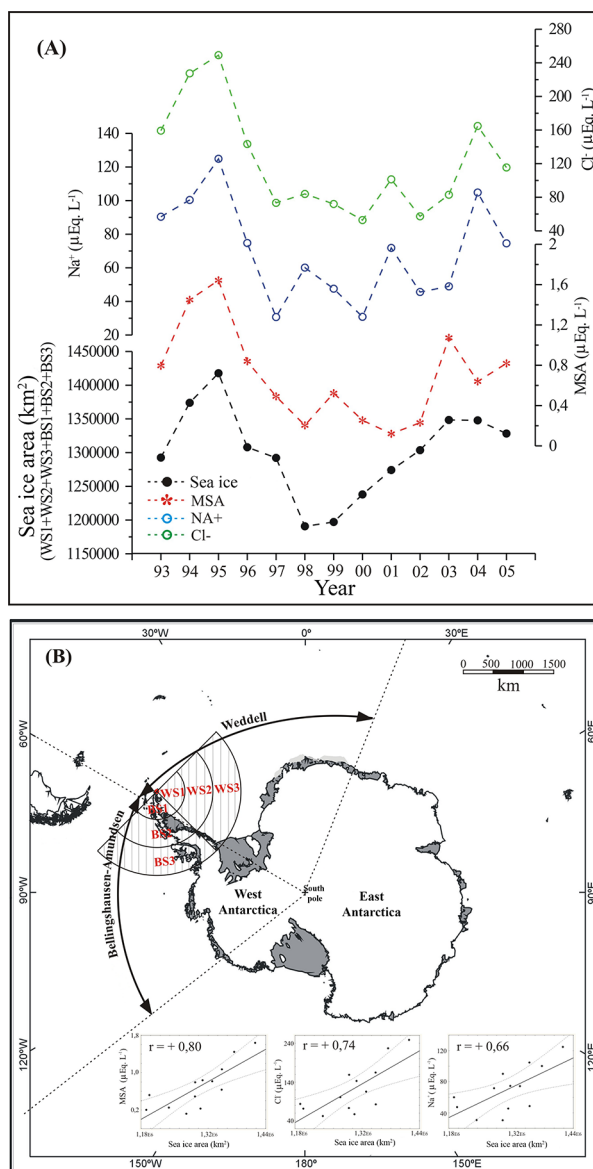


Figure 12. a) Variations of the mean annual concentration of MSA, Na^+ , and Cl^- ($\mu\text{Eq L}^{-1}$) on Joinville Island and the annual mean sea ice area of sector WS1+WS2+WS3+BS1+BS2+BS3 (km^2) from 1993 to 2005. b) Map of the Antarctic Continent showing the Weddell and ABS (dotted lines) and the corresponding sector WS1+WS2+WS3+BS1+BS2+BS3 (hatched area). The correlations between the sea ice area of the hatched region and the elements MSA, Cl^- , and Na^+ are also shown, highlighting Pearson's r value ($n = 13$, $\alpha < 0.05$).

Island from 1973 to 1988. In this study, the authors suggest that the extent of sea ice could act as a barrier to marine aerosols. Despite the low correlation value (r -Pearson = -0.43) found,

according to the authors, it falls within the limit of statistical significance (95% confidence level).

The use of Cl^- as a consistent marker of marine aerosols has been discussed in various studies conducted mainly in the central Antarctic region as depositional and post-depositional processes, such as exchange reactions between sulfuric acid and NaCl and re-emission of HCl, are well known in this region (Benassai et al. 2005, Fattori et al. 2005, Röthlisberger et al. 2003, Wagenbach et al. 1998). However, there is still a lack of studies addressing this issue in the northern Antarctic Peninsula region. Additionally, this debate should consider the hypothesis of Rankin et al. (2002), suggesting that, instead of open water, the sea ice surface would be the main source term for elements in local marine aerosols. This occurs due to the formation of fragile ice crystals known as frost flowers, which grow on the sea ice surface and can represent the main source of marine aerosols in polar areas (Kaleschke et al. 2004, Wolff 2003), whereas the structures have high salinity due to their high concentrations of Na^+ and bromide (Br^-).

CONCLUSIONS

Glaciochemical analysis of two shallow snow/firn cores from Joinville Island provided initial insights into past sea ice variability and primary productivity in the Northern Antarctic Peninsula region. The TG1 core, the longer snow/firn core, represented 13 years (1993–2005) of net accumulation ($0.4 \text{ m y}^{-1} \text{ w.eq.}$). Its chronology could only be achieved by the simultaneous observations of near-seasonal variations of $\delta^{18}\text{O}$, Na^+ and SO_4^{2-} . Additionally, the use of the ratio $\text{Mg}^{2+}/\text{Ca}^{2+}$ were critical to characterize melting effects over the cores. The description of multiple ice layers with a variety of firn grain sizes, ice lenses, depth hoar crystals in the TG1

core depicted a scenario of post-depositional processes such as melting, percolation and refreezing, leading to a partial loss of the original snow chemistry. We attribute these observations to the low elevation of the Joinville Island ice cap, at a higher altitude of only 565 m inserted in an environment that experiences temperatures above the melting point every summer season. The ionic composition of the snow/firn cores were consist to major composition of seawater and the regional biogenic activity: Cl^- (TG1 = $127.4 \mu\text{Eq L}^{-1}$ and TG2 = $87.6 \mu\text{Eq L}^{-1}$), Na^+ (TG1 = $73.9 \mu\text{Eq L}^{-1}$, TG2 = $52.4 \mu\text{Eq L}^{-1}$), K^+ (TG1 and TG2 = $2.7 \mu\text{Eq L}^{-1}$), Ca^{2+} (TG1 = $5.8 \mu\text{Eq L}^{-1}$, TG2 = $4.5 \mu\text{Eq L}^{-1}$), MSA (TG1 = $0.7 \mu\text{Eq L}^{-1}$, TG2 = $0.3 \mu\text{Eq L}^{-1}$) and F^- (TG1 and TG2 = $0.1 \mu\text{Eq L}^{-1}$).

Despite the of post-depositional processes detected at both cores, MSA and Cl^- correlated significantly with respect to sea ice, considering both the Weddell and Amundsen-Bellingshausen Sea sub-sectors ($r=0.80$ and $r=0.74$, respectively). Na^+ also correlated with both wind strength and sea ice extent ($r=0.59$ and $r=0.66$, respectively). Sectors of the Weddell and Amundsen-Bellingshausen seas, south of latitude 60°S , where correlations were higher, are consistent with prevailing wind directions obtained *in situ* by the research team. Therefore, despite the challenging process of interpreting the glaciochemical record of Joinville Island our findings highlight the role of MSA as a regional potential proxy for sea ice variability at the North Antarctica Peninsula. Thus, we believe that the results obtained here can contribute to expanding the scientific debate on the using MSA as an indirect indicator of sea ice variability in the Antarctic Continent.

Acknowledgments

We would like to thank the coordination of the Programa Antártico Brasileiro (PROANTAR), composed of the Conselho Nacional de Desenvolvimento Científico e Tecnológico (CNPq), the Ministério do Meio Ambiente

(MMA), and Marinha do Brasil, for the necessary infrastructure to carry out the work in the Antarctic region, as well as for the financial support to the Atmosphere-Ice Relationship project (no. 55.0353/2002-0). We also acknowledge the Fundação Coordenação de Aperfeiçoamento de Pessoal de Nível Superior (CAPES) for the doctoral scholarships in Brazil and abroad (PDEE - "sandwich" scholarship) and the laboratories where the analyses were performed: Laboratoire de Glaciologie et Géophysique de l'Environnement (LGGE), Institut des Géosciences de l'Environnement (IGE), Laboratoire des Sciences du Climat et de l'Environnement (LSCE), and Laboratório de Radioecologia e Mudanças Globais (LARAMG).

REFERENCES

- ABNT. 1996. NBR 13700: Áreas limpas - Classificação e controle de contaminação. Rio de Janeiro. Available at: <https://www.normas.com.br/visualizar/abnt-nbr-nm/10183/abnt-nbr13700-areas-limpas-classificacao-e-controle-de-contaminacao>.
- ABRAM NJ, MULVANEY R & ARROWSMITH C. 2011. Environmental signals in a highly resolved ice core from James Ross Island, Antarctica. *J Geophys Res* 116(D20): D20116. doi:10.1029/2011JD016147.
- ABRAM NJ, WOLFF EW & CURRAN MAJ. 2013. A review of sea ice proxy information from polar ice cores. *Quat Sci Rev* 79: 168-183. doi:10.1016/j.quascirev.2013.01.011.
- ALLEY RB, ANANDAKRISHNAN S & JUNG P. 2001. Stochastic resonance in the North Atlantic. *Paleoceanography* 16(2): 190-198. doi:10.1029/2000PA000518.
- ANDREA MO & CRUTZEN PJ. 1997. Atmospheric Aerosols: Biogeochemical Sources and Role in Atmospheric Chemistry. *Science* 276(5315): 1052-1058. doi:10.1126/science.276.5315.1052.
- ARISTARAIN AJ & DELMAS RJ. 2002. Snow chemistry measurements on James Ross Island (Antarctic Peninsula) showing sea-salt aerosol modifications. *Atmos Environ* 36(4): 765-772.
- ARISTARAIN AJ, DELMAS RJ & STIEVENARD M. 2004. Ice-core study of the link between sea-salt aerosol, sea-ice cover and climate in the Antarctic Peninsula area. *Clim Change* 67(1): 63-86.
- ARRIGO KR & VAN DIJKEN GL. 2003. Phytoplankton dynamics within 37 Antarctic coastal polynya systems. *J Geophys Res Oceans* 108(C8): 1-18. doi:10.1029/2002JC001739.
- ARRIGO KR & VAN DIJKEN GL. 2015. Continued increases in Arctic Ocean primary production. *Prog Oceanogr* 136: 60-70. doi:10.1016/j.pocean.2015.05.002.
- ARRIGO KR, VAN DIJKEN GL, CASTELAO RM, LUO H, RENNERMÄLM ÅK, TEDESCO M, MOTE TL, OLIVER HR & YAGER PL. 2017. Melting glaciers stimulate large summer phytoplankton blooms in southwest Greenland waters. *Geophys Res Lett* 44(12): 6278-6285. doi:10.1002/2017GL073583.
- ARRIGO KR ET AL. 2012. Massive Phytoplankton Blooms Under Arctic Sea Ice. *Science* 336(6087): 1408-1408. doi:10.1126/science.1215065.
- BECAGLI S ET AL. 2019. Biogenic Aerosol in the Arctic from Eight Years of MSA Data from Ny Ålesund (Svalbard Islands) and Thule (Greenland). *Atmosphere* 10(7): 1-12. doi:10.3390/atmos10070349.
- BENASSAI S, BECAGLI S, GRAGNANI R, MAGAND O, PROPOSITO M, FATTORI I, TRAVERSI R & UDISTI R. 2005. Sea-spray deposition in Antarctic coastal and plateau areas from ITASE traverses. *Ann Glaciol* 41: 32-40.
- BENMERGUI J, SHARMA S, WEN D & LIN JC. 2012. Quantitative Attribution of Processes Affecting Atmospheric Chemical Concentrations by Combining a Time-Reversed Lagrangian Particle Dispersion Model and a Regression Approach. In: *Lagrangian Modeling of the Atmosphere*. AGU 200: 251-264. doi:10.1029/2012GM001254.
- CURRAN MA, VAN OMMEN TD, MORGAN VI, PHILLIPS KL & PALMER AS. 2003. Ice core evidence for Antarctic sea ice decline since the 1950s. *Science* 302(5648): 1203-1206.
- DANSGAARD W. 1964. Stable isotopes in precipitation. *Tellus* 16(4): 436-468.
- DIGBY PGN & KEMPTON RA. 2012. *Multivariate Analysis of Ecological Communities*. Springer Science & Business Media, vol. 5, 204 p.
- DIXON D, MAYEWSKI PA, KASPARI S, KREUTZ K, HAMILTON G, MAASCH K, SNEED SB & HANDLEY MJ. 2005. A 200-year sulfate record from 16 Antarctic ice cores and associations with Southern Ocean sea-ice extent. *Ann Glaciol* 41: 155-166.
- DUCKLOW HW, BAKER K, MARTINSON DG, QUETIN LB, ROSS RM, SMITH RC, STAMMERJOHN SE, VERNET M & FRASER W. 2007. Marine pelagic ecosystems: the West Antarctic Peninsula. *Philos Trans R Soc B Biol Sci* 362(1477): 67-94. doi:10.1098/rstb.2006.1955.
- EICKEN H. 1993. The role of sea ice in structuring Antarctic ecosystems. In: Hempel G (Ed), *Weddell Sea Ecology*, Springer, p. 3-13. doi:10.1007/978-3-642-77595-6_1.
- FALKOWSKI PG, BARBER RT & SMETACEK V. 1998. *Biogeochemical Controls and Feedbacks on Ocean*

- Primary Production. *Science* 281(5374): 200-206. doi:10.1126/science.281.5374.200.
- FATTORI I, BECAGLI S, BELLANDI S, CASTELLANO E, INNOCENTI M, MANNINI A, SEVERI M, VITALE V & UDISTI R. 2005. Chemical composition and physical features of summer aerosol at Terra Nova Bay and Dome C, Antarctica. *J Environ Monit* 7(12): 1265-1274.
- GRANNAS AM, JONES AE, DIBB J, AMMANN M, ANASTASIO C, BEINE HJ, BERGIN M, BOTTENHEIM J, BOXE CS & CARVER G. 2007. An overview of snow photochemistry: evidence, mechanisms and impacts. *Atmospheric Chem Phys* 7(16): 4329-4373.
- HAMMER Ø & HARPER DA. 2001. Past: paleontological statistics software package for education and data analysis. *Palaeontol Electron* 4(1): 1.
- IIZUKA Y, IGARASHI M, KAMIYAMA K, MOTOYAMA H & WATANABE O. 2002. Ratios of Mg²⁺/Na⁺ in snowpack and an ice core at Austfonna ice cap, Svalbard, as an indicator of seasonal melting. *J Glaciol* 48(162): 452-460.
- IPCC – INTERGOVERNMENTAL PANEL ON CLIMATE CHANGE. 2022. *Climate Change 2022: Mitigation of Climate Change- Contribution of Working Group III to the Sixth Assessment Report of the Intergovernmental Panel on Climate Change*: Cambridge University Press, Cambridge, UK and New York, 2042 p. doi:10.1017/9781009157926.
- JENA B, BAJISH CC, TURNER J, RAVICHANDRAN M, ANILKUMAR N & KSHITIJIA S. 2022. Record low sea ice extent in the Weddell Sea, Antarctica in April/May 2019 driven by intense and explosive polar cyclones. *Npj Clim Atmospheric Sci* 5(1): 1-15. doi:10.1038/s41612-022-00243-9.
- JIAHONG W, JIANCHENG K, JIANKANG H, ZICHU X, LEIBAO L & DALI W. 1998. Glaciological studies on the King George Island ice cap, South Shetland Islands, Antarctica. *Ann Glaciol* 27: 105-109.
- JIANKANG H, ZICHU X, XINPING Z, DONGSHENG D, MAYEWSKI PA & TWICKLER MS. 2001. Methanesulfonate in the firn of King George Island, Antarctica. *J Glaciol* 47(159): 589-594.
- JIN M, DEAL C, WANG J, ALEXANDER V, GRADINGER R, SAITOH S, IIDA T, WAN Z & STABENO P. 2007. Ice-associated phytoplankton blooms in the southeastern Bering Sea. *Geophys Res Lett* 34(6). doi:10.1029/2006GL028849.
- JOHNSON JS & JEN CN. 2023. Role of Methanesulfonic Acid in Sulfuric Acid–Amine and Ammonia New Particle Formation. *ACS Earth Space Chem* 7(3): 653-660. doi:10.1021/acsearthspacechem.3c00017.
- KALESCHKE L ET AL. 2004. Frost flowers on sea ice as a source of sea salt and their influence on tropospheric halogen chemistry. *Geophys Res Lett* 31(16): 1-4. doi:10.1029/2004GL020655.
- KAWAGUCHI S, ISHIDA A, KING R, RAYMOND B, WALLER N, CONSTABLE A, NICOL S, WAKITA M & ISHIMATSU A. 2013. Risk maps for Antarctic krill under projected Southern Ocean acidification. *Nat Clim Change* 3(9): 843-847. doi:10.1038/nclimate1937.
- KAWAGUCHI S, KASAMATSU N, WATANABE S, ODATE T, FUKUCHI M & NICOL S. 2005. Sea ice changes inferred from methanesulphonic acid (MSA) variation in East Antarctic ice cores: are krill responsible? *Antarct Sci* 17(2): 211-212. doi:10.1017/S0954102005002610.
- KWONG KC, CHIM MM, HOFFMANN EH, TILGNER A, HERRMANN H, DAVIES JF, WILSON KR & CHAN MN. 2018. Chemical Transformation of Methanesulfonic Acid and Sodium Methanesulfonate through Heterogeneous OH Oxidation. *ACS Earth Space Chem* 2(9): 895-903. doi:10.1021/acsearthspacechem.8b00072.
- LEGRAND MR & DELMAS RJ. 1988. Formation of HCl in the Antarctic atmosphere. *J Geophys Res Atmospheres* 93(D6): 7153-7168. doi:10.1029/JD093iD06p07153.
- LEGRAND M, DUCROZ F, WAGENBACH D, MULVANEY R & HALL J. 1998. Ammonium in coastal Antarctic aerosol and snow: Role of polar ocean and penguin emissions. *J Geophys Res Atmospheres* 103(D9): 11043-11056. doi:10.1029/97JD01976.
- LEGRAND M & MAYEWSKI P. 1997. Glaciochemistry of polar ice cores: A review. *Rev Geophys* 35(3): 219-243.
- LEGRAND M & PASTEUR EC. 1998. Methane sulfonic acid to non-sea-salt sulfate ratio in coastal Antarctic aerosol and surface snow. *J Geophys Res Atmospheres* 103(D9): 10991-11006.
- LEGRAND M, WELLER R, PREUNKERT S & JOURDAIN B. 2021. Ammonium in Antarctic Aerosol: Marine Biological Activity Versus Long Range Transport of Biomass Burning. *Geophys Res Lett* 48(11): e2021GL092826. doi:10.1029/2021GL092826.
- LOWE AT, ROSS RM, QUETIN LB, VERNET M & FRITSEN CH. 2012. Simulating larval Antarctic krill growth and condition factor during fall and winter in response to environmental variability. *Mar Ecol Prog Ser* 452: 27-43. doi:10.3354/meps09409.
- LOWRY KE ET AL. 2018. Under-Ice Phytoplankton Blooms Inhibited by Spring Convective Mixing in Refreezing Leads. *J Geophys Res Oceans* 123(1): 90-109. doi:10.1002/2016JC012575.
- MARBOUTI M ET AL. IN PRESS. Relationships linking satellite-retrieved ocean color data with atmospheric

components in the Arctic. *Atmospheric Chem Phys Discuss*, p. 1-35. doi:10.5194/acp-2022-52.

MASSOM RA & STAMMERJOHN SE. 2010. Antarctic sea ice change and variability – Physical and ecological implications. *Polar Sci* 4(2): 149-186. doi:10.1016/j.polar.2010.05.001.

MAYEWSKI PA ET AL. 1994. Changes in Atmospheric Circulation and Ocean Ice Cover over the North Atlantic During the Last 41,000 Years. *Science* 263(5154): 1747-1751. doi:10.1126/science.263.5154.1747.

MCCONNELL JR, ARISTARAIN AJ, BANTA JR, EDWARDS PR & SIMÕES JC. 2007. 20th-Century doubling in dust archived in an Antarctic Peninsula ice core parallels climate change and desertification in South America. *Proc Natl Acad Sci* 104(14): 5743-5748. doi:10.1073/pnas.0607657104.

MEREDITH MP & KING JC. 2005. Rapid climate change in the ocean west of the Antarctic Peninsula during the second half of the 20th century. *Geophys Res Lett* 32(19): 1-5.

MING Y. 1997. A preliminary study on oxygen isotope of ice cores of Collins Ice Cap, King George Island, Antarctica. *Chin J Polar Sci* 8(1-English): 65-71.

MISHRA P, PANDEY CM, SINGH U, GUPTA A, SAHU C & KESHRI A. 2019. Descriptive statistics and normality tests for statistical data. *Ann Card Anaesth* 22(1): 67.

MONTES-HUGO M, DONEY SC, DUCKLOW HW, FRASER W, MARTINSON D, STAMMERJOHN SE & SCHOFIELD O. 2009. Recent Changes in Phytoplankton Communities Associated with Rapid Regional Climate Change Along the Western Antarctic Peninsula. *Science* 323(5920): 1470-1473. doi:10.1126/science.1164533.

MÜLLER E, VON GUNTEN U, BOUCHET S, DROZ B & WINKEL LHE. 2019. Hypobromous Acid as an Unaccounted Sink for Marine Dimethyl Sulfide? *Environ Sci Technol* 53(22): 13146-13157. doi:10.1021/acs.est.9b04310.

MULVANEY R, ABRAM NJ, HINDMARSH RCA, ARROWSMITH C, FLEET L, TRIEST J, SIME LC, ALEMANY O & FOORD S. 2012. Recent Antarctic Peninsula warming relative to Holocene climate and ice-shelf history. *Nature* 489(7414): 141-144. doi:10.1038/nature11391.

PARISH TR & CASSANO JJ. 2003. The role of katabatic winds on the Antarctic surface wind regime. *Mon Weather Rev* 131(2): 317-333.

RANKIN AM, WOLFF EW & MARTIN S. 2002. Frost flowers: Implications for tropospheric chemistry and ice core interpretation. *J Geophys Res Atmospheres* 107(D23): AAC-4-1-AAC 4-15. doi:10.1029/2002JD002492.

RASMUSSEN FR, KUBEČKA J & ELM J. 2022. Contribution of Methanesulfonic Acid to the Formation of Molecular Clusters in the Marine Atmosphere. *J Phys Chem A* 126(40): 7127-7136. doi:10.1021/acs.jpca.2c04468.

READ KA ET AL. 2008. DMS and MSA measurements in the Antarctic Boundary Layer: impact of BrO on MSA production. *Atmospheric Chem Phys* 8(11): 2985-2997. doi:10.5194/acp-8-2985-2008.

ROBERTS SJ ET AL. 2017. Past penguin colony responses to explosive volcanism on the Antarctic Peninsula. *Nat Commun* 8(1): 14914. doi:10.1038/ncomms14914.

RÖTHLISBERGER R, MULVANEY R, WOLFF EW, HUTTERLI MA, BIGLER M, DE ANGELIS M, HANSSON ME, STEFFENSEN JP & UDISTI R. 2003. Limited dechlorination of sea-salt aerosols during the last glacial period: Evidence from the European Project for Ice Coring in Antarctica (EPICA) Dome C ice core. *J Geophys Res Atmospheres* 108(D16): 4526. doi:10.1029/2003JD003604.

SANDS M, NICOL S & MCMINN A. 1998. Fluoride in Antarctic marine crustaceans. *Mar Biol* 132: 591-598.

SEVERI M, BECAGLI S, FROSINI D, MARCONI M, TRAVERSI R & UDISTI R. 2014. A Novel Fast Ion Chromatographic Method for the Analysis of Fluoride in Antarctic Snow and Ice. *Environ Sci Technol* 48(3): 1795-1802. doi:10.1021/es404126z.

SHAPIRO SS & WILK MB. 1965. An analysis of variance test for normality (complete samples). *Biometrika* 52(3/4): 591-611.

SIGL M, MCCONNELL JR, TOOHEY M, CURRAN M, DAS SB, EDWARDS R, ISAKSSON E, KAWAMURA K, KIPFSTUHL S & KRÜGER K. 2014. Insights from Antarctica on volcanic forcing during the Common Era. *Nat Clim Change* 4(8): 693-697.

SIMÕES J, FERRON F, BERNARDO R, ARISTARAIN A, STIÉVENARD M, POURCHET M & DELMAS R. 2004. Ice core study from King George Island, South Shetlands, Antarctica. *Pesqui Antártica Bras* 4: 9-23.

SVENSSON A ET AL. 2006. The Greenland Ice Core Chronology 2005, 15–42ka. Part 2: comparison to other records. *Quat Sci Rev* 25(23): 3258-3267. doi:10.1016/j.quascirev.2006.08.003.

THOMAS ER, ALLEN CS, ETOURNEAU J, KING ACF, SEVERI M, WINTON VHL, MUELLER J, CROSTA X & PECK VL. 2019. Antarctic Sea Ice Proxies from Marine and Ice Core Archives Suitable for Reconstructing Sea Ice over the Past 2000 Years. *Geosciences* 9(12): 506. doi:10.3390/geosciences9120506.

THOMAS ER, BRACEGIRDLE TJ, TURNER J & WOLFF EW. 2013. A 308-year record of climate variability in West Antarctica. *Geophys Res Lett* 40(20): 5492-5496. doi:10.1002/2013GL057782.

THOMAS ER ET AL. 2023. Ice core chemistry database: an Antarctic compilation of sodium and sulfate records spanning the past 2000 years. *Earth Syst Sci Data* 15(6): 2517-2532. doi:10.5194/essd-15-2517-2023.

TRUSEL LD, FREY KE, DAS SB, MUNNEKE PK & VAN DEN BROEKE MR. 2013. Satellite-based estimates of Antarctic surface meltwater fluxes. *Geophys Res Lett* 40(23): 6148-6153.

TURNER J, HOLMES C, CATON HARRISON T, PHILLIPS T, JENA B, REEVES-FRANCOIS TT, FOGT R, THOMAS ER & BAJISH CC. 2022. Record low Antarctic sea ice cover in February 2022. *Geophys Res Lett* 49(12): e2022GL098904.

TURNER J, LU H, WHITE I, KING JC, PHILLIPS T, HOSKING JS, BRACEGIRDLE TJ, MARSHALL GJ, MULVANEY R & DEB P. 2016. Absence of 21st century warming on Antarctic Peninsula consistent with natural variability. *Nature* 535(7612): 411-415. doi:10.1038/nature18645.

VAUGHAN DG, MARSHALL GJ, CONNOLLEY WM, PARKINSON C, MULVANEY R, HODGSON DA, KING JC, PUDSEY CJ & TURNER J. 2003. Recent Rapid Regional Climate Warming on the Antarctic Peninsula. *Clim Change* 60(3): 243-274. doi:10.1023/A:1026021217991.

VINTHER BM, CLAUSEN HB, JOHNSEN SJ, RASMUSSEN SO, ANDERSEN KK, BUCHARDT SL, DAHL-JENSEN D, SEIERSTAD IK, SIGGAARD-ANDERSEN ML & STEFFENSEN JP. 2006. A synchronized dating of three Greenland ice cores throughout the Holocene. *J Geophys Res Atmospheres* 111(D13): 1-11.

WAGENBACH D, DUCROZ F, MULVANEY R, KECK L, MINIKIN A, LEGRAND M, HALL JS & WOLFF EW. 1998. Sea-salt aerosol in coastal Antarctic regions. *J Geophys Res Atmospheres* 103(D9): 10961-10974. doi:10.1029/97JD01804.

WANG J, LUO H, YANG Q, LIU J, YU L, SHI Q & HAN B. 2022. An unprecedented record low Antarctic sea-ice extent during austral summer 2022. *Adv Atmos Sci* 39(10): 1591-1597.

WELCH KA, MAYEWSKI PA & WHITLOW SI. 1993. Methanesulfonic acid in coastal Antarctic snow related to sea-ice extent. *Geophys Res Lett* 20(6): 443-446.

WOLFF EW. 2003. Whither Antarctic sea ice? *Science* 302(5648): 1164-1164.

WOLFF EW, BARBANTE C, BECAGLI S, BIGLER M, BOUTRON CF, CASTELLANO E, DE ANGELIS M, FEDERER U, FISCHER H & FUNDEL F. 2010. Changes in environment over the last 800,000 years from chemical analysis of the EPICA Dome C ice core. *Quat Sci Rev* 29(1-2): 285-295.

YU J, TIAN JY, ZHANG ZY, YANG GP, CHEN HJ, XU R & CHEN R. 2019. Role of *Calanus sinicus* (Copepoda, Calanoida) on Dimethylsulfide and Dimethylsulfoniopropionate

Production in Jiaozhou Bay. *J Geophys Res Biogeosciences* 124(8): 2481-2498. doi:10.1029/2018JG004721.

ZEMP M E AL. 2019. Global glacier mass changes and their contributions to sea-level rise from 1961 to 2016. *Nature* 568(7752): 382-386. doi:10.1038/s41586-019-1071-0.

SUPPLEMENTARY MATERIAL

Table S1.
Figure S1.

How to cite

DE ALENCAR AS, EVANGELISTA H, GONÇALVES JR SJ, SIMÕES JC, FELZENSZWALB I, SETZER A & PASSOS HR. 2024. On the potential of glaciochemical analysis of Joinville Island firn core for the sea ice reconstruction around the northern Antarctic Peninsula. *An Acad Bras Cienc* 96: e20230751. DOI 10.1590/0001-3765202420230751.

Manuscript received on July 8, 2023;
accepted for publication on October 8, 2024

ALEXANDRE S. DE ALENCAR¹

<https://orcid.org/0000-0002-8104-1781>

HEITOR EVANGELISTA²

<https://orcid.org/0000-0001-9832-1141>

SÉRGIO J. GONÇALVES JR²

<https://orcid.org/0000-0002-1852-0894>

JEFFERSON C. SIMÕES^{3,4}

<https://orcid.org/0000-0001-5555-3401>

ISRAEL FELZENSZWALB⁵

<https://orcid.org/0000-0003-1677-197X>

ALBERTO SETZER⁶

<https://orcid.org/0000-0002-2466-7366>

HEBER R. PASSOS⁶

<https://orcid.org/0009-0003-7290-4631>

¹Universidade Veiga de Almeida, Departamento de Ciências Biológicas, Rua Ibituruna, 108, Maracanã, 20271-110 Rio de Janeiro, RJ, Brazil

²Universidade do Estado do Rio de Janeiro (UERJ), Laboratório de Radioecologia e Mudanças Globais (LARAMG), Rua São Francisco Xavier, 524, Pavilhão Haroldo Lisboa da Cunha, Subsolo, Maracanã, 20550-013 Rio de Janeiro, RJ, Brazil

³Universidade Federal do Rio Grande do Sul (UFRGS), Instituto de Geociências, Av. Bento Gonçalves, 9500, Agronomia, 91501-970 Porto Alegre, RS, Brazil

⁴University of Maine, Climate Change Institute, 16-40 Grove St Ext, Orono, ME, 4469-5790, USA

⁵Universidade do Estado do Rio de Janeiro (UERJ), Laboratório de Mutagênese Ambiental, Departamento de Biofísica e Biometria (DBB), Av. Boulevard 28 de Setembro, 87, 4º andar, Vila Isabel, 20551-030 Rio de Janeiro, RJ, Brazil

⁶Instituto Nacional de Pesquisas Espaciais (INPE), Av. dos Astronautas, 1758, Jardim da Granja, 12227-010 São José dos Campos, SP, Brazil

Correspondence to: **Sérgio J. Gonçalves Jr**

E-mail: sjrgoncalves@gmail.com

Author contributions

A.S.A., H.E. conducted the project, leading the conceptualization, methodology, sampling, formal analysis, investigation and final review; S.J.G.Jr. writing of original draft, conducted scientific discussions, final review & final editing; J.C.S. conducted sampling, writing of original draft and final review; I.F. conducted formal analysis and investigation; A.S., H.R.P. conducted meteorological analyses and sampling.

